Environ Health Prev Med (2008) 13:25–29
DOI 10.1007/s12199-007-0007-8

Epigenetic abnormalities in cardiac hypertrophy and heart failure

Hiroyuki Mano

Received: 23 June 2007 / Accepted: 4 August 2007 / Published online: 11 December 2007

Abstract Epigenetics refers to the heritable regulation of gene expression through modification of chromosomal components without an alteration in the nucleotide sequence of the genome. Such modifications include methylation of genomic DNA as well as acetylation, methylation, phosphorylation, ubiquitination, and SUMOylation of core histone proteins. Recent genetic and biochemical analyses indicate that epigenetic changes play an important role in the development of cardiac hypertrophy and heart failure, with dysregulation in histone acetylation status, in particular, shown to be directly linked to an impaired contraction ability of cardiac myocytes. Although such epigenetic changes should eventually lead to alterations in the expression of genes associated with the affected histones, little information is yet available on the genes responsible for the development of heart failure. Current efforts of our and other groups have focused on deciphering the network of genes which are under abnormal epigenetic regulation in failed hearts. To this end, coupling chromatin immunoprecipitation to high-throughput profiling systems is being applied to cardiac myocytes in normal as well as affected hearts. The results of these studies should not only improve our understanding of the molecular basis for cardiac hypertrophy/heart failure but also provide essential information that will facilitate the development of new epigenetics-based therapies.

H. Mano (✉)
Division of Functional Genomics, Jichi Medical University,
3311-1 Yakushiji, Shimotsuke, Tochigi 329-0498, Japan
e-mail: hmano@jichi.ac.jp

Keywords Cardiac hypertrophy · Chromatin immunoprecipitation · Heart failure · Histone acetylation · Subtraction

What is "epigenetics"?

The eukaryotic genome is tightly compacted as a result of its association with highly conserved histone proteins. The interaction of stretches of genomic DNA with core histone proteins (two molecules each of H2A, H2B, H3, and H4) thus results in the formation of nucleosomes, which are the basic structural units of chromatin. The further association of histone H1 and other proteins with nucleosomes strengthens the compaction and gives rise to the highly ordered, condensed structure of the chromosome (Fig. 1). The interaction of genomic DNA with these chromosomal proteins greatly influences the access of transcriptional factors to their target DNA sequences and thereby regulates transcriptional activity.

"Epigenetics" refers to the heritable regulation of gene expression through the modification of chromosomal components without an alteration in the nucleotide sequence of the genome [1]. Several such modifications have been linked to the regulation of gene expression, including methylation of genomic DNA as well as acetylation, methylation, phosphorylation, ubiquitination, and sumoylation of histone proteins (Fig. 1).

Core histones have an amino-terminal tail that protrudes from the chromatin fiber and which is believed to interact with DNA or other histone or modulatory proteins. Lysine and arginine residues within this tail are the main targets for histone modification. Lysine-9 in histone H3 (H3-K9), for example, becomes methylated or acetylated in response to a variety of signals. In general, the acetylation of

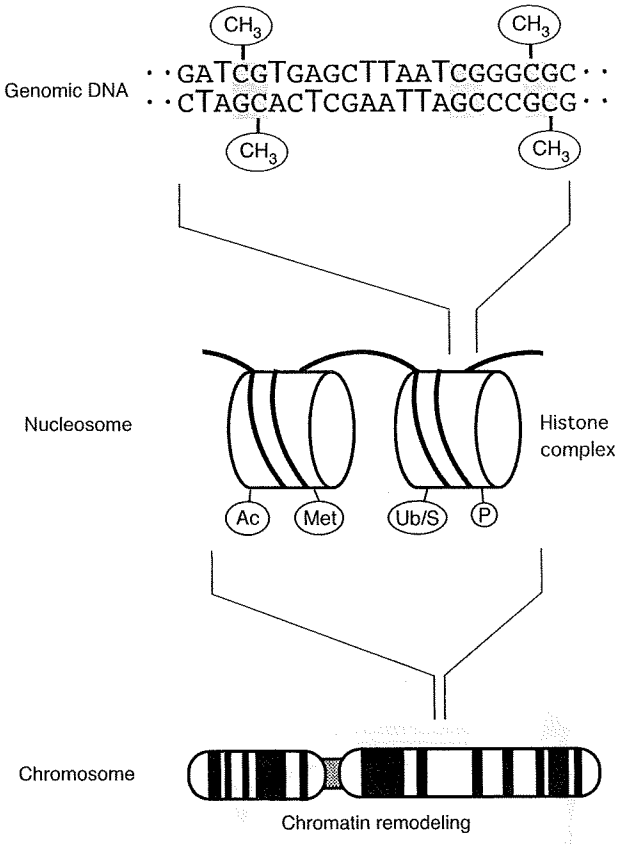

Fig. 1 Epigenetic changes at different levels of chromatin structure. CpG sites within genomic DNA undergo methylation, and core histones in nucleosomes undergo acetylation (*Ac*), methylation (*Met*), ubiquitination (*Ub*), sumoylation (*S*), or phosphorylation (*P*). Higher order chromatin structure is also dynamically modified by chromatin-remodeling complexes

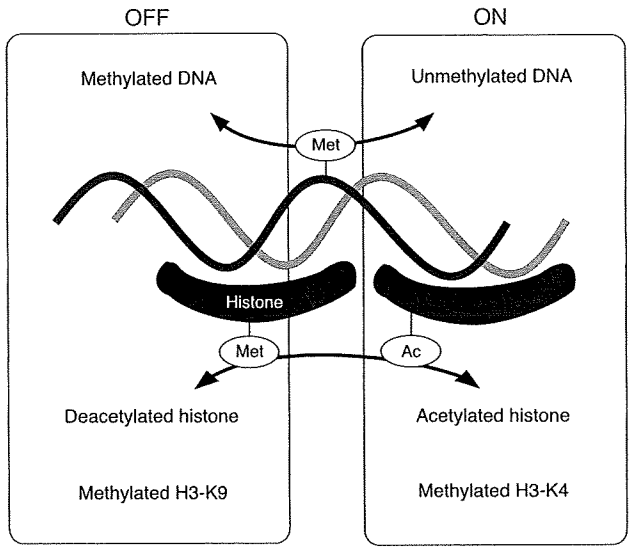

Fig. 2 Epigenetic changes and transcriptional activity. Suppression of gene expression (*OFF*) is correlated with the methylation (*Met*) of genomic DNA, deacetylation of histones, and methylation of H3-K9. In contrast, activation of gene expression (*ON*) is associated with unmethylated genomic DNA, acetylated (*Ac*) histones, and methylated H3-K4

histones is associated with the induction of gene expression (Fig. 2). The acetylation of histone tails is thought to neutralize the positive charge of lysine residues and thereby to induce a decondensation of chromatin structure. The resulting open architecture of the chromosome allows transcriptional factors to access their binding sites in genomic DNA and to activate transcription. However, the same histone modification has been associated with seemingly diverse outputs in a context-dependent manner. The existence of a "histone code" has thus been proposed, with a combination of histone modifications – and not only one – supposedly specifying the outcome in terms of gene expression [2]. However, this hypothesis has been challenged by recent data [3].

The acetylation of histone tails is mediated by histone acetyltransferases (HATs), whose activity in cells is rapidly counteracted by that of histone deacetylases (HDACs) [4]. The turnover time of histone acetylation in cells is thus as short as a few minutes [5]. The importance of histone acetylation in the regulation of gene expression has been demonstrated for a variety of cellular processes, including cell differentiation, cell cycle progression, DNA repair, and carcinogenesis [6, 7].

Epigenetic status in cardiac myocytes

The regulation of histone acetylation has been shown to be linked to cardiac hypertrophy. The HAT activity of CREB-binding protein (CBP) and p300 is thus required for the induction of hypertrophic changes in cardiac muscle cells by phenylephrine [8]. Consistent with this observation, the inhibition of HDAC activity results in an increase in the size of muscle cells [9]. Furthermore, class II HDACs (HDAC4, -5, -7, and -9) suppress cardiac hypertrophy, in part by binding to and inhibiting the activity of myocyte enhancer factor 2 (MEF2) [10]. In contrast, however, HDAC2 together with Hop, a homeodomain protein, was found to promote cardiac hypertrophy in vivo in a manner sensitive to systemic administration of the HDAC inhibitor trichostatin A (TSA) [11]. Moreover, HDAC inhibitors prevent hypertrophy and sarcomere organization in cultured cardiac myocytes [12], which is suggestive of a positive role for HDACs in cardiac hypertrophy.

These seemingly discrepant findings may be attributable either to differential actions of different classes of HDACs (and, possibly, of HATs) with regard to myocyte hypertrophy or to a dissociation between the deacetylase activity of HDACs and a pro-hypertrophic function [10]. Clarification of the role of HATs and HDACs in hypertrophy

would be facilitated by the identification of the genes targeted by these enzymes during the induction of hypertrophic changes. Little is known, however, of the genes regulated by HATs or HDACs in myocytes. Induction of the atrial natriuretic peptide (ANP) gene is associated with the acetylation of histones (H3 and H4) located in the 3′ untranslated region of the gene [13]. Histones bound to the β-myosin heavy chain gene have also been shown to be targeted by HATs in myocytes [10].

Differential chromatin scanning (DCS) method

Given the essential role of histone acetylation in cardiac hypertrophy, it is important that the genes or genome regions bound to histones with such differential modifications be identified. Chromatin immunoprecipitation (ChIP) coupled with hybridization to genome tiling microarrays ("ChIP-on-chip" experiments) has been used to screen for those genes under epigenetic regulation [14–16]. However, an extensive mapping of ChIP products on the human genome has been hampered by insufficient information on human genome annotation. Furthermore, hybridization of genome-derived fragments to microarrays is prone to non-specific signals that partly represent the GC contents of the fragments.

To effectively isolate genome fragments with differential epigenetic regulation, we have developed a novel "DCS" method which basically couples ChIP to subtraction PCR [17, 18]. The DCS procedure is schematically shown in Fig. 3. Following the cross-linking of DNA to histones through the use of formaldehyde, both tester and driver cells are separately lysed and subjected to mild DNA shearing by sonication for a short period. Complexes of DNA and acetylated histones are then specifically immunoprecipitated with antibodies to acetylated histone H3, after which the DNA fragments are released from such complexes into solution.

The nonspecific binding of residual RNA is then minimized by treating the DNA solution with RNase A, and the DNA fragments are then blunt-ended. The DNA is digested maximally with *Rsa*I to obtain fragments with a relatively uniform size of several hundred base pairs. A TAG adaptor is ligated to both ends of the DNA fragments, and subsequent PCR amplification with a TAG primer yields amplicons with an *Xma*I/*Sma*I site at each end.

The tester DNA is then digested with *Xma*I (thereby generating cohesive ends), whereas the driver DNA is digested with *Sma*I (generating blunt ends). The tester DNA is ligated with the first subtraction adaptor [19] at its cohesive ends and is then annealed to an excess amount of the driver DNA. Under this condition, DNA fragments present only in the tester sample undergo self-annealing and thereby generate a binding site for the first subtraction

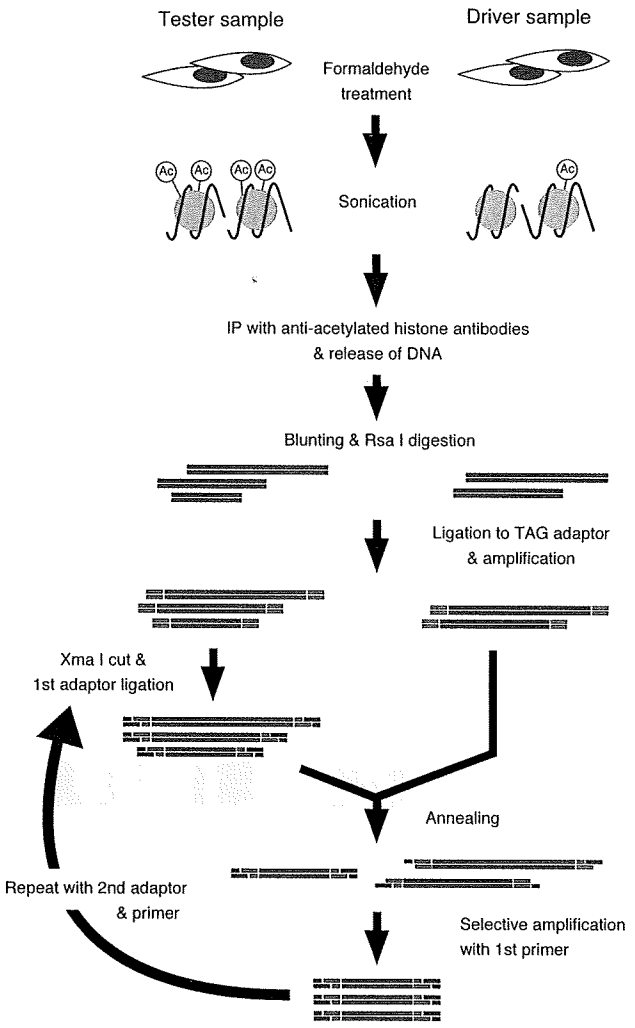

Fig. 3 The differential chromatin scanning (DCS) method. DNA fragments bound to acetylated (*Ac*) histones are purified by immunoprecipitation (*IP*) and subjected to TAG adaptor ligation (*green bars*) and PCR amplification. The tester DNA is then digested with *Xma*I, ligated to the first subtraction adaptor (*red bars*), and annealed with an excess amount of the driver DNA. Given that only the tester-specific fragments self-anneal, PCR with the first subtraction primer selectively amplifies these fragments. The products are subjected to a second round of subtraction PCR with the second subtraction adaptor and primer to ensure the fidelity of the subtraction. Reproduced from Kaneda et al. [17]

primer at both ends. Subsequent PCR amplification with this primer thus selectively amplify the tester-specific DNA fragments [17].

To exclude DNA fragments that possess endogenous (probably nonspecific) binding sites for the first subtraction primer, we then digest the first subtraction products with *Xma*I and ligate the resulting molecules with the second subtraction adaptor. A second round of subtraction amplification is then performed with the second subtraction primer, yielding DNA fragments that are associated with acetylated histones, specifically in the tester cells [17].

To verify the fidelity of DCS, we attempted to isolate genome fragments which are the targets of HDAC in cardiac myocytes. A rat cardiomyocyte cell line, H9C2, was treated with TSA and was used as the tester, while the cells without the TSA treatment was used as the driver. Differential chromatin scanning was applied to this pair of cells and subsequently identified hundreds of genome fragments that could be immunoprecipitated by antibodies to acetylated histones only in the tester cells.

Some of the clones thus identified correspond to loci within or close to rat genes whose products function in intracellular calcium mobilization or antioxidant processes. One such clone, H9C2T-2_D09, mapped to a region encompassing intron 21 and exon 22 of *Itpr3* (Fig. 4a), which encodes a receptor for inositol 1,4,5-trisphosphate that plays an important role in Ca^{2+}-mediated signal transduction [18]. The cytosolic concentration of Ca^{2+} directly regulates muscle contraction and cardiac rhythm and is a determinant of myocyte hypertrophy and heart failure [20]. The amount of the genomic fragment corresponding to the H9C2T-2_D09 clone was 6.6-fold greater in the ChIP product of TSA-treated cells than in that of untreated cells (Fig. 4b), indicating that the extent of histone acetylation in this region of the genome of the tester cells was 6.6-fold that in the driver cells. Furthermore, inhibition of HDAC activity was accompanied by an increase in the amount of *Itpr3* mRNA [18] (Fig. 4c). These data suggest that HDAC actively deacetylates a chromosomal region corresponding to *Itpr3* and thereby suppresses the transcriptional activity of the gene.

To visualize directly the genome-wide distribution of HDAC targets, we mapped the DCS genomic clones whose chromosomal positions were known to rat chromosome figures (Fig. 5). The HDAC targets were distributed widely throughout the rat genome, although some "hot spots" for deacetylation were apparent. For example, seven of the DCS clones mapped to chromosomal position 5q36, and detailed mapping revealed that all of these clones were located within a region spanning 27 Mbp. It is thus possible that regional alterations of chromatin structure result in coordinated transcriptional regulation of genes within the affected region.

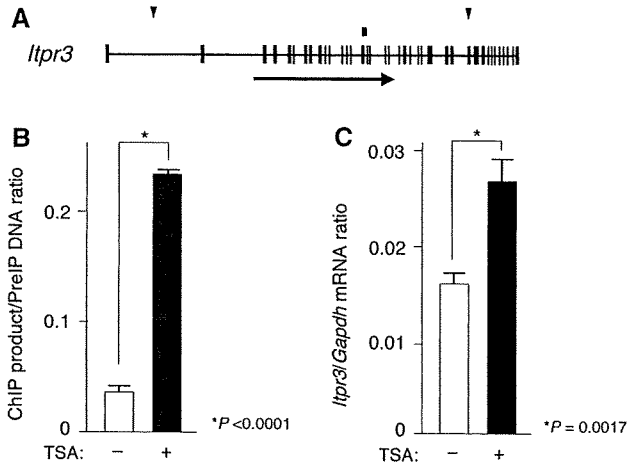

Fig. 4 Identification of *Itpr3* as a target of histone deacetylase (HDAC) in cardiomyocytes. **a** One of the DCS clones (H9C2T-2_D09; *red rectangle*) was mapped to chromosome 20p12, spanning intron 21 and exon 22 of *Itpr3*. Exons are denoted by *black boxes*, the *arrow* indicates the direction of transcription, and *blue triangles* depict distance markers separated by 50 kbp. **b** Chromatin immunoprecipitates were prepared from H9C2 cells treated (+) or not (−) with 300 n*M* inhibitor trichostatin A (TSA) for 24 h. The amount of DNA corresponding to the H9C2T-2_D09 sequence in each chromatin immunoprecipitation (*ChIP*) product relative to that in the corresponding original sample before immunoprecipitation (*PreIP*) was then determined by real-time PCR. **c** The amount of *Itpr3* mRNA relative to that of *Gapdh* mRNA in H9C2 cells treated or not with TSA was determined by quantitative reverse transcription (RT)-PCR. All data are means ± SD of triplicates from representative experiments that were performed at least twice. *P* values for the indicated comparisons were determined by Student's *t* test. Reproduced from Kaneda et al. [18]

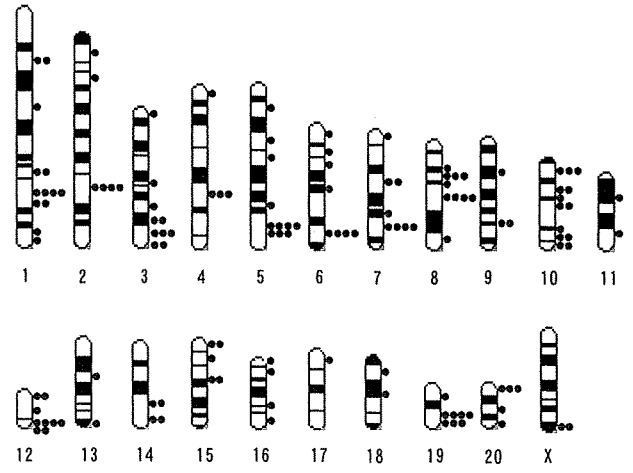

Fig. 5 Chromosomal distribution of HDAC targets. The genome fragments (*red dots*) isolated by the DCS method were mapped to rat chromosomes. Reproduced from Kaneda et al. [18]

Future directions

As described herein, cells manifest numerous types of epigenetic modifications, including acetylation and methylation, on core histone proteins. Although the results of biochemical and genetic studies suggest that histone acetylation plays an important role in the development of cardiac hypertrophy/heart failure (at least, in mouse), it is an open question whether changes in the other epigenetic marks are essential or, rather, causative of the heart disorders. An analysis of human heart specimens would be of particular great value.

In terms of technology development, DCS is not free from disadvantages. Although DCS can isolate genome fragments that are the recipients differential regulation of any epigenetic marks (provided specific antibodies are available), it does not measure the extent of "differential regulation". In other words, DCS is more a qualitative approach than a quantitative one. Several high-throughput sequencing technologies are currently emerging which simultaneously provide sequence information for millions of clones [21]. Coupling such sequencing system to ChIP would be one of the ideal ways to quantitatively measure epigenetic modifications: (1) frequency in the read data would be a surrogate marker for the intensity of epigenetic modifications; (2) sequence information of the reads would be useful to map such reads onto human genome.

It is apparent that epigenetic change is the key event in the development of cardiac hypertrophy/heart failure. Analysis of human specimens with emerging technologies would substantially facilitate researchers in their efforts to pinpoint the causative genes for these disorders.

References

1. Egger G, Liang G, Aparicio A, Jones PA. Epigenetics in human disease and prospects for epigenetic therapy. Nature. 2004;429:457–63.
2. Strahl BD, Allis CD. The language of covalent histone modifications. Nature. 2000;403:41–5.
3. Dion MF, Altschuler SJ, Wu LF, Rando OJ. Genomic characterization reveals a simple histone H4 acetylation code. Proc Natl Acad Sci USA. 2005;102:5501–6.
4. Verdin E, Dequiedt F, Kasler HG. Class II histone deacetylases: versatile regulators. Trends Genet. 2003;19:286–93.
5. Waterborg JH. Dynamics of histone acetylation in vivo. A function for acetylation turnover? Biochem Cell Biol. 2002;80:363–78.
6. Kouzarides T. Histone acetylases and deacetylases in cell proliferation. Curr Opin Genet Dev. 1999;9:40–8.
7. Yasui W, Oue N, Ono S, Mitani Y, Ito R, Nakayama H. Histone acetylation and gastrointestinal carcinogenesis. Ann NY Acad Sci. 2003;983:220–31.
8. Gusterson RJ, Jazrawi E, Adcock IM, Latchman DS. The transcriptional co-activators CREB-binding protein (CBP) and p300 play a critical role in cardiac hypertrophy that is dependent on their histone acetyltransferase activity. J Biol Chem. 2003;278:6838–47.
9. Iezzi S, Di Padova M, Serra C, Caretti G, Simone C, Maklan E, et al. Deacetylase inhibitors increase muscle cell size by promoting myoblast recruitment and fusion through induction of follistatin. Dev Cell. 2004;6:673–84.
10. Zhang CL, McKinsey TA, Chang S, Antos CL, Hill JA, Olson EN. Class II histone deacetylases act as signal-responsive repressors of cardiac hypertrophy. Cell. 2002;110:479–88.
11. Kook H, Lepore JJ, Gitler AD, Lu MM, Wing-Man Yung W, Mackay J, et al. Cardiac hypertrophy and histone deacetylase-dependent transcriptional repression mediated by the atypical homeodomain protein Hop. J Clin Invest. 2003;112:863–71.
12. Antos CL, McKinsey TA, Dreitz M, Hollingsworth LM, Zhang CL, Schreiber K, et al. Dose-dependent blockade to cardiomyocyte hypertrophy by histone deacetylase inhibitors. J Biol Chem. 2003;278:28930–7.
13. Kuwahara K, Saito Y, Ogawa E, Takahashi N, Nakagawa Y, Naruse Y, et al. The neuron-restrictive silencer element-neuron-restrictive silencer factor system regulates basal and endothelin 1-inducible atrial natriuretic peptide gene expression in ventricular myocytes. Mol Cell Biol. 2001;21:2085–97.
14. Weinmann AS, Yan PS, Oberley MJ, Huang TH, Farnham PJ. Isolating human transcription factor targets by coupling chromatin immunoprecipitation and CpG island microarray analysis. Genes Dev. 2002;16:235–44.
15. Ballestar E, Paz MF, Valle L, Wei S, Fraga MF, Espada J, et al. Methyl-CpG binding proteins identify novel sites of epigenetic inactivation in human cancer. EMBO J. 2003;22:6335–45.
16. Odom DT, Zizlsperger N, Gordon DB, Bell GW, Rinaldi NJ, Murray HL, et al. Control of pancreas and liver gene expression by HNF transcription factors. Science. 2004;303:1378–81.
17. Kaneda R, Toyota M, Yamashita Y, Koinuma K, Choi YL, Ota J, et al. High-throughput screening of genome fragments bound to differentially acetylated histones. Genes Cells. 2004;9:1167–74.
18. Kaneda R, Ueno S, Yamashita Y, Choi YL, Koinuma K, Takada S, et al. Genome-wide screening for target regions of histone deacetylases in cardiomyocytes. Circ Res. 2005;97:210–8.
19. Toyota M, Ho C, Ahuja N, Jair KW, Li Q, Ohe-Toyota M, et al. Identification of differentially methylated sequences in colorectal cancer by methylated CpG island amplification. Cancer Res. 1999;59:2307–12.
20. Marks AR. Cardiac intracellular calcium release channels: role in heart failure. Circ Res. 2000;87:8–11.
21. Service RF. Gene sequencing. The race for the $1000 genome. Science. 2006;311:1544–6.

Environ Health Prev Med (2008) 13:30–35
DOI 10.1007/s12199-007-0004-y

REVIEW

Epidemiological approach to nosocomial infection surveillance data: the Japanese Nosocomial Infection Surveillance System

Machi Suka · Katsumi Yoshida · Jun Takezawa

Received: 11 May 2007 / Accepted: 9 August 2007 / Published online: 11 December 2007

Abstract Surveillance of nosocomial infection is the foundation of infection control. Nosocomial infection surveillance data ought to be summarized, reported, and fed back to health care personnel for corrective action. Using the Japanese Nosocomial Infection Surveillance (JANIS) data, we determined the incidence of nosocomial infections in intensive care units (ICUs) of Japanese hospitals and assessed the impact of nosocomial infections on mortality and length of stay. We also elucidated individual and environmental factors associated with nosocomial infections, examined the benchmarking of infection rates and developed a practical tool for comparing infection rates with case-mix adjustment. The studies carried out to date using the JANIS data have provided valuable information on the epidemiology of nosocomial infections in Japanese ICUs, and this information will contribute to the development of evidence-based infection control programs for Japanese ICUs. We conclude that current surveillance systems provide an inadequate feedback of nosocomial infection surveillance data and, based on our results, suggest a methodology for assessing nosocomial infection surveillance data that will allow infection control professionals to maintain their surveillance systems in good working order.

Keywords Epidemiology · Intensive care units · Japan · Nosocomial infections · Surveillance

Introduction

Infection control in the hospital setting is performed with the aim of improving the effectiveness of patient care and promoting patient safety. Infection control professionals need to recognize and explain nosocomial infections and design and implement interventions to reduce their incidence. These infection control activities should have their bases in a well-designed surveillance system of nosocomial infections [1].

Compared with the USA and other developed countries, Japan traditionally had limited sources of information on the epidemiology of nosocomial infections and, until recently, little was known about the incidence and outcome of nosocomial infections in Japanese hospitals. The Japanese Ministry of Health, Labour, and Welfare established the Japanese Nosocomial Infection Surveillance (JANIS) system in July 2000, when participating hospitals routinely started to collect and subsequently make their nosocomial infection surveillance data available for entry into a national database. The JANIS database has now become the most important source of information on the epidemiology of nosocomial infections in Japanese hospitals.

In the study reported here, we used the JANIS data to determine the incidence of nosocomial infections in intensive care units (ICUs) of Japanese hospitals and assess the impact of nosocomial infections on mortality and length of stay. We elucidated individual and environmental

This article is based upon the research that was given encouragement award at the 77th annual meeting of the Japanese Society for Hygiene held in Osaka, Japan on 25–28 March 2007.

M. Suka (✉) · K. Yoshida
Department of Preventive Medicine, St Marianna University School of Medicine, 2-16-1 Sugao, Miyamae-ku Kawasaki, Kanagawa 216-8511, Japan
e-mail: suka@marianna-u.ac.jp

J. Takezawa
Department of Emergency and Intensive Care Medicine, Nagoya University Graduate School of Medicine, Nagoya, Japan

bjh research paper

Functional analysis of *JAK3* mutations in transient myeloproliferative disorder and acute megakaryoblastic leukaemia accompanying Down syndrome

Tomohiko Sato,[1] Tsutomu Toki,[1] Rika Kanezaki,[1] Gang Xu,[1] Kiminori Terui,[1] Hirokazu Kanegane,[2] Masayoshi Miura,[3] Souichi Adachi,[4] Masahiro Migita,[5] Shingo Morinaga,[6] Takahide Nakano,[7] Mikiya Endo,[8] Seiji Kojima,[9] Hitoshi Kiyoi,[10] Hiroyuki Mano[11] and Etsuro Ito[1]

[1]Department of Paediatrics, Hirosaki University Graduate School of Medicine, Hirosaki, [2]Department of Paediatrics, Graduate School of Medicine, University of Toyama, Toyama, [3]Department of Paediatrics, Toyama City Hospital, Toyama, [4]Department of Paediatrics, Graduate School of Medicine, Kyoto University, Kyoto, [5]Department of Paediatrics, Japan Red Cross Kumamoto Hospital, Kumamoto, [6]Department of Paediatrics, National Hospital Organization Kumamoto Medical Centre, Kumamoto, [7]Department of Paediatrics, Kansai Medical University, Osaka, [8]Department of Paediatrics, Iwate Medical University, Morioka, [9]Department of Paediatrics, Nagoya University Graduate School of Medicine, Nagoya, [10]Department of Infectious Diseases, Nagoya University Graduate School of Medicine, Nagoya, and [11]Division of Functional Genomics, Jichi Medical University, Shimotsuke, Japan

Summary

JAK3 mutations have been reported in transient myeloproliferative disorder (TMD) as well as in acute megakaryoblastic leukaemia of Down syndrome (DS-AMKL). However, functional consequences of the *JAK3* mutations in TMD patients remain undetermined. To further understand how *JAK3* mutations are involved in the development and/or progression of leukaemia in Down syndrome, additional TMD patients and the DS-AMKL cell line MGS were screened for *JAK3* mutations, and we examined whether each *JAK3* mutation is an activating mutation. *JAK3* mutations were not detected in 10 TMD samples that had not previously been studied. Together with our previous report we detected *JAK3* mutations in one in 11 TMD patients. Furthermore, this study showed for the first time that a TMD patient-derived *JAK3* mutation ($JAK3^{I87T}$), as well as two novel *JAK3* mutations ($JAK3^{Q501H}$ and $JAK3^{R657Q}$) identified in an MGS cell line, were activating mutations. Treatment of MGS cells and Ba/F3 cells expressing the JAK3 mutants with JAK3 inhibitors significantly decreased their growth and viability. These results suggest that the *JAK3* activating mutation is an early event during leukaemogenesis in Down syndrome, and they provide proof-of-principle evidence that JAK3 inhibitors would have therapeutic effects on TMD and DS-AMKL patients carrying activating *JAK3* mutations.

Keywords: Down syndrome, transient myeloproliferative disorder, acute megakaryoblastic leukaemia, JAK3, STAT5.

Received 14 November 2007; accepted for publication 2 January 2008
Correspondence: Etsuro Ito, Department of Paediatrics, Hirosaki University Graduate School of Medicine, Hirosaki, Aomori, 036-8563 Japan. E-mail: eturou@cc.hirosaki-u.ac.jp

Down syndrome (DS), which is caused by trisomy 21, is one of the most common human chromosomal abnormalities. Children with DS have an approximately 20-fold higher incidence of leukaemia than the general population (Hitzler & Zipursky, 2005). The majority of leukaemia cases associated with DS are acute megakaryoblastic leukaemia (AMKL). Approximately 10% of infants with DS develop a postnatal transient myeloproliferative disorder (TMD), which is characterized by rapid growth of abnormal blast cells with erythroid-megakaryocytic phenotype (Ito *et al*, 1995). Although the majority of TMD cases resolve spontaneously, AMKL develops in approximately 20% of TMD cases in the first four years of life. Recently, we and others demonstrated that acquired mutations of the *GATA1* gene were detected in almost all cases

 First published online 7 April 2008
British Journal of Haematology, **141**, 681–688 doi:10.1111/j.1365-2141.2008.07081.x

of DS-related AMKL (DS-AMKL) and TMD (Wechsler *et al*, 2002; Groet *et al*, 2003; Hitzler *et al*, 2003; Mundschau *et al*, 2003; Rainis *et al*, 2003; Xu *et al*, 2003; Ahmed *et al*, 2004). In each case, the mutation resulted in the introduction of a premature stop codon in the gene sequence encoding the N-terminal activation domain, leading to expression of an alternative 40-kD translation product (GATA1s) from a downstream initiation site.

The available evidence indicates that an acute leukaemia would arise from cooperation between one class of mutations that interferes with differentiation, such as loss-of-function mutations in haematopoietic transcription factors, and a second class of mutations that confers a proliferative advantage to cells, such as activating mutations in the haematopoietic tyrosine kinases (Deguchi & Gilliland, 2002). Indeed, Walters *et al* (2006) reported gain-of-function mutations of the *JAK3* gene in the DS-AMKL cell line CMK, and in one of three DS-AMKL patients, all of who also had *GATA1* mutations. These mutations consisted of A572V and V722I substitutions, which both occur in the JH2 pseudokinase domain. All JAK3 mutants constitutively activated and transformed Ba/F3 cells to factor-independent growth.

Recently, we identified a *JAK3* mutation in one of two TMD patients that were screened (Kiyoi *et al*, 2007). However, the functional consequences and frequency of the *JAK3* mutations in TMD patients remain undetermined. To further understand how *JAK3* mutations are involved in the development and/or progression of leukaemia in DS, we screened additional TMD patients as well as the DS-AMKL cell line MGS for *JAK3* mutations, and we examined whether each *JAK3* mutation is an activation mutation. *JAK3* mutations occurred in TMD patients at a low frequency, similar to that found earlier in DS-AMKL. Furthermore, we show for the first time that the previously identified $JAK3^{I87T}$ mutation associated with TMD, as well as two novel *JAK3* mutations ($JAK3^{Q501H}$ and $JAK3^{R657Q}$) identified in MGS cells, were activating mutations. Treatment of MGS cells and Ba/F3 cells expressing the JAK3 mutants with JAK3 inhibitors resulted in a significant decrease in their growth and viability. These results suggest that *JAK3* activating mutation is an early event during the development of AMKL in DS, and they provide proof-of-principle evidence that JAK3 inhibitors would have therapeutic effects on AMKL and TMD patients carrying activating *JAK3* mutations.

Materials and methods

Patients and cell lines

This study was approved by the Ethics Committee of Hirosaki University Graduate School of Medicine, and all clinical samples were obtained with informed consent. The MGS cell line was established from leukaemic cells obtained from a patient with DS-AMKL. This cell line was a gift from Dr. Mitsui (Yamagata University School of Medicine). The K562 cell line was established from leukaemic cells that were obtained from a patient with chronic myeloid leukaemia. These cell lines were cultured in RPMI 1640 medium (Sigma, St Lois, MO, USA) supplemented with 10% fetal bovine serum (Gibco BRL, Rockville, MD, USA). Ba/F3 cells were obtained from the Japanese Center Resources Bank and were cultured in RPMI 1640 medium supplemented with 10% fetal bovine serum and 1 ng/ml recombinant murine interleukin (IL)-3 (Kirin Brewery, Tokyo, Japan). PLAT-E, the retrovirus packaging cell line, was kindly provided by Dr Kitamura (the University of Tokyo; Morita *et al*, 2000). This cell line was cultured in Dulbecco's modified Eagle's medium (DMEM; Gibco BRL) supplemented with 10% fetal bovine serum and 1 μg/ml puromycin, 10 μg/ml brastidine, 50 U/ml penicillin and 50 μg/ml streptomycin. All cell lines were maintained at 37°C and in 5% CO_2 atmosphere.

Analysis of JAK3 mutations

To analyse *JAK3* mutation in clinical samples, total RNA was isolated from peripheral blood or bone marrow cells using an ISOGEN kit (Wako, Osaka, Japan) and was reverse transcribed using random hexamers. The synthesized cDNA were amplified using a ligation-anchored polymerase chain reaction (LA PCR) kit (TaKaRa, Ohtsu, Japan) and direct sequencing was performed by means of the ABI PRISM Bigdye Terminator Cycle Sequencing Ready Reaction Kit (Applied Biosystems, Foster City, CA, USA). The primers used in this analysis are shown in Table SI. To analyse *JAK1* mutation in MGS cells, direct sequence analysis for the entire coding sequences was performed using cDNA.

Construction of retroviral vectors

To establish each retroviral expression vector, the pMX-ires-CD8 plasmid vector (Yamashita *et al*, 2001) was used. The wild type *JAK3* cDNA was ligated into the *Eco*RI site of pMX-ires-CD8 to produce pMX-ires-CD8-$JAK3^{WT}$. The other retroviral expression vectors, pMX-ires-CD8-$JAK3^{Q501H}$, pMX-ires-CD8-$JAK3^{R657Q}$, pMX-ires-CD8-$JAK3^{Q501H\ and\ R657Q}$, pMX-ires-CD8-$JAK3^{A572V}$ and pMX-ires-CD8-$JAK3^{V674A}$ were generated from pMX-ires-CD8-$JAK3^{WT}$ by PCR.

Ba/F3 cell transformation assay

PLAT-E cells were transfected with plasmid DNA using the Fugene transfection kit (Roche, Basel, Switzerland). Retroviral supernatants were collected 72 h after transfection and incubated with Ba/F3 cells for 24 h in the RetroNectin Dish (TaKaRa). To obtain the transduced cells, CD8-positive cells were selected using a MACS Separation Column (Miltenyi Biotec, Bergisch Gladbach, Germany) and expanded. Finally, we confirmed the transductions by detecting CD8-positive cells using fluorescence-activated cell sorting (FACS).

Cell proliferation assay

Ba/F3 cells expressing JAK3 mutants were incubated in the absence of IL-3 for 7–8 days. Viable cell number was determined every 1–2 days using Cell Counting Kit 8 (Wako, Osaka, Japan), according to the manufacturer's recommendations.

Immunoblot analysis

Before obtaining whole-cell extracts, Ba/F3 cells were cultured in serum-free RPMI 1640 medium for 4 h and then incubated in medium with 10% fetal bovine serum for 5 min. The whole-cell extracts were separated on SDS-PAGE and transferred to Hybond-P membranes (Amersham Biosciences, Little Chalfont, UK). Immunodetections were carried out using anti-phospho-STAT5 (Cell Signalling, Danvers, MA, USA) and anti-STAT5 antibodies (Santa Cruz Biotechnology, Santa Cruz, CA, USA). Dilutions were 1:1000 and 1:500 respectively. The signals were visualized with anti-rabbit horseradish peroxidase conjugates (GE Healthcare UK LTD, Buckinghamshire, England) and enhanced chemiluminescence (ECL) plus Western blotting detection reagents (Amersham Biosciences).

JAK inhibitors assay

For the purpose of the inhibitor analysis, Ba/F3 cells expressing various JAK3 mutants were cultured for 10 days in the absence of IL-3. These cells were treated with increasing concentrations of WHI-P131 (JAK3 inhibitor I) and WHI-P154 (JAK3 inhibitor II). After 48 h, the viable cell number was determined using Cell Counting Kit 8.

Results

JAK3 mutations in the DS-AMKL cell line MGS

To investigate the role of the JAK/STAT pathway in DS-associated leukaemogenesis, we first examined the effects of a pan-JAK inhibitor on the growth and viability of the DS-AMKL cell line MGS. Treatment with the pan-JAK inhibitor (JAK inhibitor I) resulted in significantly decreased cell proliferation and viability (Fig 1A). This effect could not be attributed to nonspecific toxicity, because growth and viability were not inhibited by pan-JAK inhibitor in K562 cells that express the BCR-ABL fusion protein. These results suggest that JAK activation was essential for growth and survival of MGS cells. Because reverse transcription (RT)-PCR analysis showed that, of the JAK family, only *JAK1* and *JAK3* were expressed in MGS cells (data not shown), we then analysed *JAK1* and *JAK3* for activating mutations. Sequence analysis identified two novel *JAK3* mutations (a Q501H substitution in the JH3 SH2 domain and an R657Q substitution in the JH2 pseudokinase domain) in MGS cells (Fig 1B and C), whereas no mutation was detected in *JAK1*. We performed RT-PCR analysis using primers corresponding to the outside of each mutation. A PCR product encompassing both mutations was

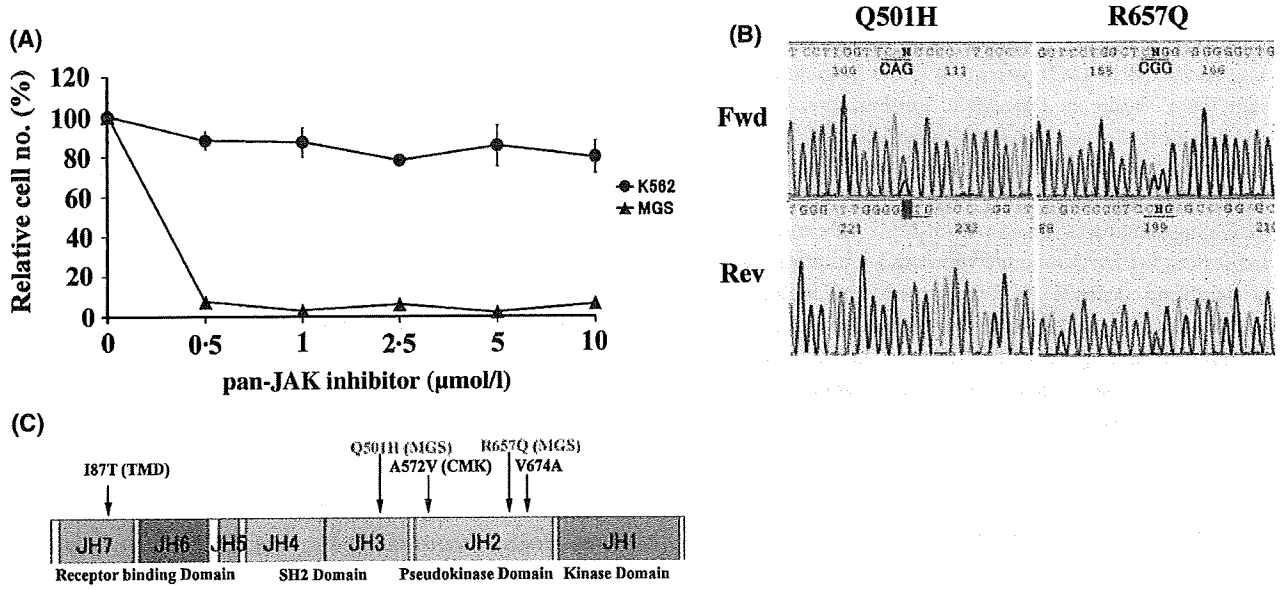

Fig 1. *JAK3* mutation in the DS-AMKL cell line MGS. (A) Treatment with the pan-JAK inhibitor (JAK inhibitor I) resulted in significantly decreased cell proliferation and viability of MGS cells, but not K562 cells that express the BCR–ABL fusion protein. Viable cell number was determined using Cell Counting Kit 8 at 72 h. Mean value ± SD of experiments performed in triplicate is represented. For each cell line, the relative cell number in presence of increasing amount of inhibitor was calculated as a percentage of control (without inhibitor). (B) Sequence analysis of the *JAK3* gene showing that MGS cells harbour two novel mutations (Q501H and R657Q) in the same allele. (C) Q501H and R657Q, indicated by red letters, were located in the JH3 SH2 domain and JH2 pseudokinase domain respectively. A572V, identified in CMK cells, and the artificially generated V674A were located in the pseudokinase domain, and the I87T associated with the TMD patient and indicated by black letters occurred in the receptor-binding domain.

cloned into plasmid pCR II (Invitrogen). Sequence analysis confirmed that the two mutations were in the same allele.

JAK3 contains a gain-of-function mutation in MGS cells

To examine the transforming ability of *JAK3*^{Q501H} and *JAK3*^{R657Q} mutations, we constructed retroviral expression vectors containing various *JAK3* mutations and transduced Ba/F3 cells with either pMX-ires-CD8-*JAK3*^{Q501H}, *JAK3*^{R657Q}, *JAK3*$^{Q501H\ and\ R657Q}$ or *JAK3*^{WT}. As positive controls, we used the expression vectors pMX-ires-CD8-*JAK3*^{A572V} for the JAK3 activating mutation identified in CMK and pMX-ires-CD8-*JAK3*^{V674A} for the artificially generated, oncogenic *JAK3* mutation (Choi *et al*, 2006; Walters *et al*, 2006). Twenty-four hours after transduction, CD8-positive cells were selected using immunobeads, cultured in the absence of IL-3, and subjected to the cell proliferation assay. As shown in Fig 2A, expression of either JAK3^{Q501H} or JAK3^{R657Q} conferred IL-3-independent growth to Ba/F3 cells, but these cells grew much more slowly than the Ba/F3 cells expressing JAK3^{V674} or JAK3^{A572V}. Interestingly, the cells transduced with pMX-ires-CD8-*JAK3*$^{Q501H\ and\ R657Q}$ grew as fast as the positive controls, suggesting that the JAK3$^{Q501H\ and\ R657Q}$ showed more potent transforming activity than did either single substitution.

Constitutive and ligand-independent activation of the downstream signalling pathway induced by JAK mutations

To analyse signalling properties of the JAK3 mutants, we next evaluated the phosphorylation status of STAT5, the downstream target of JAK3. Western blot analysis of Ba/F3 cells revealed that STAT5 was constitutively phosphorylated in cells transduced with JAK3$^{Q501H\ and\ R657Q}$ or with JAK3^{V674} or JAK3^{A572V}, but not in cells transduced with JAK^{WT}. STAT5 phosphorylation was also detected in cells transduced with JAK3^{Q501H} or JAK3^{R657Q}, but this effect was very weak compared with JAK3$^{Q501H\ and\ R657Q}$ (Fig 2B). These results suggest that the transforming activity is correlated with the kinase activity of each JAK3 mutant protein.

JAK3 mutation identified in a TMD patient

We previously found *JAK3* mutations in one of two TMD and one of 11 DS-AMKL patients (Kiyoi *et al*, 2007). The A573V and A593T substitutions, which occur in the same allele and which both are in the JH2 pseudokinase domain, were found in the one affected DS-AMKL patient, while the affected TMD patient had an I87T substitution in the JH7 receptor-binding domain. Of note, the fact that the *JAK3* mutation was found in a TMD patient indicated that this is an early event during the development of AMKL in DS. However, the frequency and functional consequences of *JAK3* mutations in TMD remain unknown because of the small sample size. We therefore screened for *JAK3* mutations in another 10 TMD patients by analysing their cDNA. Direct sequence analysis revealed no *JAK3* mutations in these patients, while *GATA1* mutations were detected in all cases (Table I). Recently, De Vita *et al* (2007) reported an acquired loss-of-function *JAK3* mutation because of a large deletion (592 bp) of a fragment encoding the JH1 kinase domain. This mutation was found in two of eight TMD patients and in one of eight DS-AMKL patients (De Vita

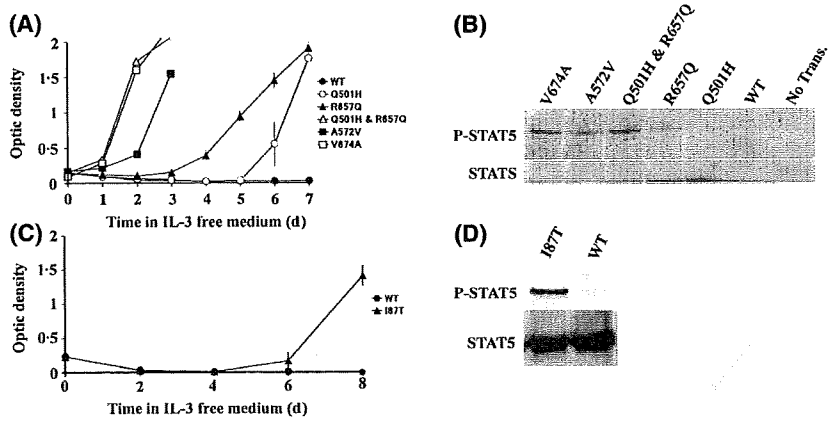

Fig 2. *JAK3* mutations from MGS cells and a TMD patient transformed Ba/F3 cells. (A) Expression of JAK3 mutants identified in MGS cells abrogated cytokine dependency of Ba/F3 cells. Ba/F3 cells were transduced with either pMX-ires-CD8-*JAK3*^{Q501H}, *JAK3*^{R657Q}, *JAK3*$^{Q501H\ and\ R657Q}$ or *JAK3*^{WT}. Positive controls were pMX-ires-CD8-*JAK3*^{A572V} for the JAK3-activating mutant identified in CMK cells and pMX-ires-CD8-*JAK3*^{V674A} for the artificially-generated oncogenic JAK3 mutant (Choi *et al*, 2006; Walters *et al*, 2006). After transduction, CD8-positive cells were selected using immunobeads, cultured at a density of 2×10^5/ml in the absence of IL-3 and evaluated by a cell proliferation assay. Values represent mean ± SD. The experiments were repeated twice, and both data sets were essentially identical. (B) *JAK3* mutations cause constitutive JAK3 activation. Ba/F3 cells were transduced with various JAK3 expression vectors, and CD8-positive cells were selected using immunobeads. Cell lysates were subjected to immunoblot analysis for phospho-STAT5 and total STAT5. (C) Ba/F3 cells were transduced with either pMX-ires-CD8-*JAK3*^{I87T} or *JAK3*^{WT}. After transduction, CD8-positive cells were selected using immunobeads, cultured at a density of 4×10^5/ml in the absence of IL-3, and evaluated by a cell proliferation assay. Values represent mean ± SD. The experiments were repeated twice, and both data sets were essentially identical. (D) Ba/F3 cells expressing JAK3^{I87T} were grown in the absence of IL-3. Lysates of Ba/F3 cells were subjected to immunoblot analysis for phospho-STAT5 or total STAT5.

Table I. Mutations of *GATA1* and *JAK3* genes in transient myeloproliferative disorder (TMD) patients.

Patients	Sex	Blast (%)	*GATA1* mutations	*JAK3* mutations
TMD-1	Male	82	Exon 2, subs 7, pos 305	Wild
TMD-2	Female	86	Exon 2, del 2, pos 202	Wild
TMD-3	Male	92	Exon 2, ins 12, pos 298	Wild
TMD-4	Male	69	Exon 2, subs (T > C) exon/intron boundary	Wild
TMD-5	Male	84	Exon 3, del 129, pos 342	Wild
TMD-6	Female	48	Exon 2, del 136, pos 94	Wild
TMD-7	Male	93	Exon 2, del 23, pos 265	Wild
TMD-8	Male	94	Exon 2, del 218, exon/intron boundary	Wild
TMD-9	Female	55	Exon 2, subs (C > G) pos 319	Wild
TMD-10	Male	60	Exon 2, del 8, pos 213	Wild

del, deletion; subs, substitution; ins, insertion.
Nucleotide position 1 is taken from GenBank sequence of human *GATA1* (NM_002049).

et al, 2007). However, we failed to detect these mutations in any of our patients.

To examine whether the $JAK3^{I87T}$ mutation identified in a TMD patient was an activating mutation, Ba/F3 cells were transduced with either pMX-ires-CD8-$JAK3^{I87T}$ or $JAK3^{WT}$. As shown in Fig 2C, expression of JAK^{I87T} conferred IL-3-independent growth to Ba/F3 cells, whereas $JAK3^{WT}$-transduced cells retained dependence on IL-3 for proliferation. However, these cells grew slower than the Ba/F3 cells expressing either $JAK3^{Q501H}$, or $JAK3^{R657Q}$ (data not shown). The constitutive phosphorylation of STAT5 was weaker in the cells expressing JAK^{I87T} than $JAK3^{Q501H}$ or $JAK3^{R657Q}$ (data not shown), and was detected only after JAK^{I87T}-transduced cells started growing in the absence of IL-3 (Fig 2D). These results suggest that $JAK3^{I87T}$ is a gain-of-function mutation, although its kinase activity was weak compared with that associated with the other JAK3 mutants.

JAK3 inhibitors affect the proliferation of cells expressing JAK3 mutants

We next assessed the effects of small molecule JAK inhibitors on the proliferation of MGS cell expressing JAK3 mutant proteins. Treatment with WHI-P154 (JAK3 inhibitor II), but not the JAK2 inhibitor AG490, resulted in significantly decreased proliferation of MGS cells compared with K562 cells (Fig 3A and B). To further study the effects of JAK3 inhibitors on each JAK3 mutant, we next examined the effects

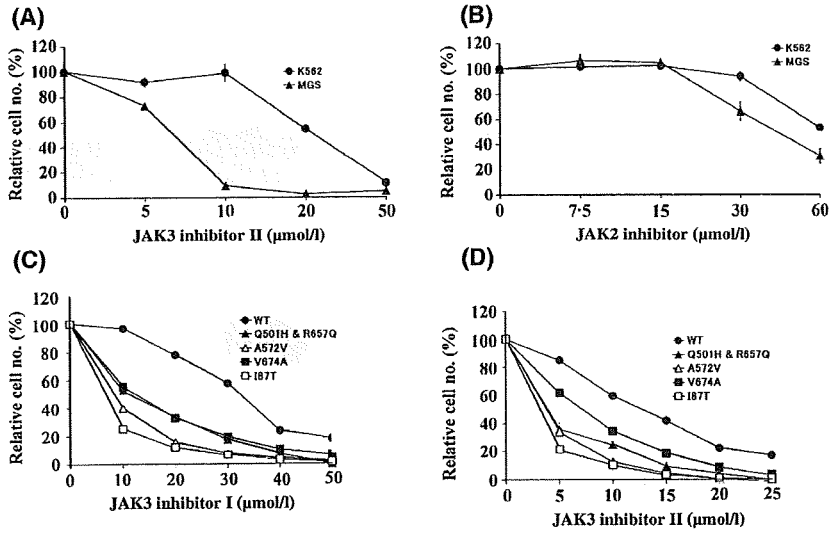

Fig 3. JAK3 inhibitors affect proliferation of cells expressing JAK3 mutants. MGS and K562 control cells were treated with increasing concentrations of WHI-P154 (JAK3 inhibitor II) (A) or JAK2 inhibitor AG490 (B). Note that treatment with WHI-P154, but not AG490, resulted in significantly decreased proliferation of MGS cells compared with K562 cells. Ba/F3 cells expressing various JAK3 mutants without added IL-3 and Ba/F3 cells expressing $JAK3^{WT}$ with added IL-3 were treated with increasing concentrations of WHI-P131 (JAK3 inhibitor I) (C) or JAK3 inhibitor II (D). Viable cell number was determined using Cell Counting Kit 8 at 48 h. Mean value ± SD of experiments performed in triplicate is represented. For each cell line, the relative cell number in presence of increasing amount of inhibitor was calculated as a percentage of control (without inhibitor). The experiments were repeated twice, and both data sets were essentially identical.

of JAK inhibitors on the Ba/F3 cells expressing each JAK3 mutant. For this analysis, Ba/F3 cells expressing various JAK3 mutants were cultured for 10 days in the absence of IL-3. These cells grew slowly at first, as shown in Fig 2A and C. However, they all started growing well in the absence of IL-3 subsequently. WHI-P131 (JAK3 inhibitor I) and JAK3 inhibitor II inhibited the proliferation of all Ba/F3 cells expressing the various JAK3 mutants in the absence of IL-3, although the sensitivities to each JAK3 inhibitor differed slightly among these Ba/F3 cells (Fig 3C and D and Fig S1). This effect could not be attributed to nonspecific toxicity, because the sensitivities to the Ba/F3 cells expressing $JAK3^{WT}$ were significantly reduced in the presence of IL-3, whose receptor utilizes JAK2 (Silvennoinen *et al*, 1993). These results confirmed that the gain-of-function mutations of *JAK3* conferred IL-3 independent growth to Ba/F3 cells.

Discussion

Analysis of TMD and DS-AMKL may provide invaluable information for understanding leukaemia pathogenesis. To further understand how *JAK3* mutations are involved in the development and/or progression of leukaemia in DS, we screened TMD patients and the DS-AMKL cell line MGS for *JAK3* mutations and examined the functional consequences of these mutations. This study showed, for the first time, that a TMD patient-derived *JAK* mutation ($JAK3^{I87T}$), as well as two novel *JAK3* mutations ($JAK3^{Q501H}$ and $JAK3^{R657Q}$) identified in an MGS cell line, were activating mutations. These results have significantly improved our understanding of the mechanisms of multi-step leukaemogenesis in DS.

Only two DS-AMKL cell lines, CMK and MGS, have been reported until now. *GATA1* mutations were detected in both of these cell lines (Xu *et al*, 2003). The results are consistent with the fact that *GATA1* mutations are detected in almost all cases with TMD and DS-AMKL. Furthermore, we identified the mutations of the *TP53* tumour suppressor genes in both of these cell lines (Kanezaki *et al*, 2006). However, the roles of *TP53* mutations in DS-AMKL remain unknown, because *TP53* mutations are rare in DS-AMKL as well as TMD (Hirose *et al*, 2003) and the inactivation of p53 is frequently observed in myeloid leukaemia cell lines. Recently, Walters *et al* (2006) first reported *JAK3* activating mutations (A572V) in CMK cells. This study identified two novel *JAK3* activating mutations (Q501H and R657Q in the same allele) in MGS cells. The fact that two out of two DS-AMKL cell lines have activating *JAK3* mutations indicates that constitutive activation of the JAK/STAT pathway may play a very important role in the development of leukaemia in DS.

An activating *JAK2* mutation affecting the pseudokinase domain ($JAK2^{V617F}$) has been observed frequently in myeloproliferative disorders (Baxter *et al*, 2005; James *et al*, 2005; Levine *et al*, 2005). In contrast to the *JAK2* mutations, *JAK3* mutations have been observed in a variety of domains including the JH2 pseudokinase domain, the JH3 SH2 domain and the JH6 and JH7 receptor binding domain (Choi *et al*, 2006; Walters *et al*, 2006; De Vita *et al*, 2007; Kiyoi *et al*, 2007). However, only four activating JAK3 mutants, including one artificially generated mutant, were verified using functional assays (Choi *et al*, 2006; Walters *et al*, 2006). Among these four mutations, three were located in the JH2 pseudokinase domain and the remaining mutation was located in the JH6 receptor-binding domain. The SH2 domain is thought to contribute to *in vivo* assembly of the JAK, but the functional role of this domain is only partly defined. This study showed, for the first time, that a mutation in the SH2 domain ($JAK3^{Q501H}$) was also an activating mutation. Interestingly, the double mutation $JAK3^{Q501H \text{ and } R657Q}$ had much more potent transforming activity than did each individual substitution, but the mechanism behind this effect remains unknown. We used the Ba/F3 transformation assay to examine whether each JAK3 mutant is an activating mutation. This is a standard assay *in vitro* but of limited value. JAK3 mutants are expressed at non-physiological levels in a myelo-lymphoid cell line rather than primary cells that have a megakaryocyte-erythroid phenotype. To further understand the roles of *JAK3* mutations in leukaemogenesis, it is necessary to express JAK3 mutants in primary bone marrow cells *in vitro* and *in vivo*.

Our findings, taken together with previous published data (Walters *et al*, 2006; De Vita *et al*, 2007; Kiyoi *et al*, 2007; Klusmann *et al*, 2007; Norton *et al*, 2007), show that the observed incidence of *JAK3* mutations in TMD and in DS-AMKL was 5/38 patients and 6/45 patients respectively. Although the incidences of *JAK3* mutations in TMD and DS-AMKL differ from reports in three other recent studies (De Vita *et al*, 2007; Klusmann *et al*, 2007; Norton *et al*, 2007), these results indicate that the frequency of *JAK3* mutations in TMD and DS-AMKL is similar. This suggests that *JAK3* mutations are very early events that can cooperate with *GATA1* mutations during the development of TMD. However, the fact that *JAK3* mutations occurred in TMD patients and in DS-AMKL patients only at a low frequency suggests that other distinct genetic changes probably contribute to the development of TMD, and to the progression to AMKL from TMD.

This study has shown for the first time that a TMD patient-derived *JAK* mutation was also an activating mutation. The N-terminal portion of the JAK3 JH5-JH7 domain, which has homology to a band four-point-one, ezrin, radixin, soesin (FERM; Girault *et al*, 1999), is required for receptor binding and maintenance of a functional kinase domain (Zhou *et al*, 2001). Severe combined immunodeficiency (SCID) patient-derived mutations within the JAK3 FERM domain impair the kinase-receptor interaction and abrogate JAK3 catalytic activity. In this study, we showed that the TMD patient-derived $JAK3^{I87T}$, which leads to an amino-acid substitution in the JH7 FERM domain, is an activating mutation, like the substitution $JAK3^{P132T}$, which was found in a non-DS-AMKL patient (Walters *et al*, 2006).

Functional analysis of *JAK3* mutations in this study indicates the possibility that *JAK3* mutations are the cause of

progression from TMD to AMKL in a subset of patients. Firstly, in MGS cells, the two individual mutations were not as potent as a combination of the two in conferring IL-3 independent growth of Ba/F3 cells (and p-STAT5 levels). This might infer that one of these mutations was present during the initial TMD phase and that it needed a second mutation, leading to a stronger JAK3 activation (higher p-STAT5), to precipitate AMKL. Secondly, the mutation detected in TMD (JAK^{I87T}) confers IL3 independent growth only weakly, whereas all mutations in AMKL show a much stronger effect. Of course, the analysis of additional *JAK3* mutations in TMD/AMKL patients will need to be conducted to substantiate or refute this claim. In particular, the analysis of sequential samples from individual TMD and AMKL patients could be very important to determine this.

JAK3 is predominantly expressed in haematopoietic cells and is specifically associated with the common γ chain (γc)-containing receptors including interleukin 2 (IL-2), IL-4, IL-7, IL-9, IL-15 and IL-21 (Miyazaki *et al*, 1994). Loss-of-function mutations of the γc chain or JAK3 result in SCID (Russell *et al*, 1995; Leonard, 2000). Targeting JAK3, therefore, would theoretically offer ideal immune suppression when it is needed without causing any effects outside of these cell populations (Borie *et al*, 2004). Recently, a more specific, potent and orally active inhibitor of JAK3 was developed. This JAK3 inhibitor, CP-690,550, produces sufficient immune suppression by itself to prevent organ transplant rejection, without inducing many of the side effects observed with current therapies (Changelian *et al*, 2003). In this study, we showed that treatment with the JAK3 inhibitor WHI-P131 (JAK3 inhibitor I) or WHI-P154 (JAK3 inhibitor II) resulted in significantly decreased growth and viability of cells expressing activating JAK3 mutants, although these compounds were less specific and potent than CP-690,550. These results provide proof-of-principle evidence that JAK3 inhibitors should have therapeutic effects for TMD and DS-AMKL patients carrying an activating *JAK3* mutation.

Acknowledgements

We thank Dr T Kitamura (the University of Tokyo) for providing a PLAT-E cell line. This work was supported by Grants-in-Aid for Scientific Research and Grants-in-Aid for Scientific Research on Priority Areas from the Ministry of Education, Science, Sports and Culture.

References

Ahmed, M., Sternberg, A., Hall, G., Thomas, A., Smith, O., O'Marcaigh, A., Wynn, R., Stevens, R., Addison, M., King, D., Stewart, B., Gibson, B., Roberts, I. & Vyas, P. (2004) Natural history of GATA1 mutations in Down syndrome. *Blood*, **103**, 2480–2489.

Baxter, E.J., Scott, L.M., Campbell, P.J., East, C., Fourouclas, N., Swanton, S., Vassiliou, G.S., Bench, A.J., Boyd, E.M., Curtin, N., Scott, M.A., Erber, W.N. & Green, A.R. (2005) Acquired mutation of the tyrosine kinase JAK2 in human myeloproliferative disorders. *The Lancet*, **365**, 1054–1061.

Borie, D.C., O'Shea, J.J. & Changelian, P.S. (2004) JAK3 inhibition, a viable new modality of immunosuppression for solid organ transplants. *Trends in Molecular Medicine*, **10**, 532–541.

Changelian, P.S., Flanagan, M.E., Ball, D.J., Kent, C.R., Magnuson, K.S., Martin, W.H., Rizzuti, B.J., Sawyer, P.S., Perry, B.D., Brissette, W.H., McCurdy, S.P., Kudlacz, E.M., Conklyn, M.J., Elliott, E.A., Koslov, E.R., Fisher, M.B., Strelevitz, T.J., Yoon, K., Whipple, D.A., Sun, J., Munchhof, M.J., Doty, J.L., Casavant, J.M., Blumenkopf, T.A., Hines, M., Brown, M.F., Lillie, B.M., Subramanyam, C., Shang-Poa, C., Milici, A.J., Beckius, G.E., Moyer, J.D., Su, C., Woodworth, T.G., Gaweco, A.S., Beals, C.R., Littman, B.H., Fisher, D.A., Smith, J.F., Zagouras, P., Magna, H.A., Saltarelli, M.J., Johnson, K.S., Nelms, L.F., Des Etages, S.G., Hayes, L.S., Kawabata, T.T., Finco-Kent, D., Baker, D.L., Larson, M., Si, M.S., Paniagua, R., Higgins, J., Holm, B., Reitz, B., Zhou, Y.J., Morris, R.E., O'Shea, J.J. & Borie, D.C. (2003) Prevention of organ allograft rejection by a specific Janus kinase 3 inhibitor. *Science*, **302**, 875–878.

Choi, Y.L., Kaneda, R., Wada, T., Fujiwara, S., Soda, M., Watanabe, H., Kurashina, K., Hatanaka, H., Enomoto, M., Takada, S., Yamashita, Y. & Mano, H. (2006) Identification of a constitutively active mutant of JAK3 by retroviral expression screening. *Leukemia Research*, **31**, 203–209.

De Vita, S., Mulligan, C., McElwaine, S., Dagna-Bricarelli, F., Spinelli, M., Basso, G., Nizetic, D. & Groet, J. (2007) Loss-of-function JAK3 mutations in TMD and AMKL of Down syndrome. *British Journal of Haematology*, **137**, 337–341.

Deguchi, K. & Gilliland, D.G. (2002) Cooperativity between mutations in tyrosine kinases and in hematopoietic transcription factors in AML. *Leukemia*, **16**, 740–744.

Girault, J., Labesse, G., Mornon, J. & Callebaut, I. (1999) The N-termini of FAK and JAKs contain divergent band 4.1 domains. *Trends in Biochemical Sciences*, **24**, 54–57.

Groet, J., McElwaine, S., Spinelli, M., Rinaldi, A., Burtscher, I., Mulligan, C., Mensah, A., Cavani, S., Dagna-Bricarelli, F., Basso, G., Cotter, F.E. & Nizetic, D. (2003) Acquired mutations in GATA1 in neonates with Down's syndrome with transient myeloid disorder. *Lancet*, **361**, 1617–1620.

Hirose, Y., Kudo, K., Kiyoi, H., Hayashi, Y., Naoe, T. & Kojima, S. (2003) Comprehensive analysis of gene alterations in acute megakaryoblastic leukemia of Down's syndrome. *Leukemia*, **17**, 2250–2252.

Hitzler, J.K. & Zipursky, A. (2005) Origins of leukaemia in children with Down syndrome. *Nature Reviews Cancer*, **5**, 11–20.

Hitzler, J.K., Cheung, J., Li, Y., Scherer, S.W. & Zipursky, A. (2003) GATA1 mutations in transient leukemia and acute megakaryoblastic leukemia of Down syndrome. *Blood*, **101**, 4301–4304.

Ito, E., Kasai, M., Hayashi, Y., Toki, T., Arai, K., Yokoyama, S., Kato, K., Tachibana, N., Yamamoto, M. & Yokoyama, M. (1995) Expression of erythroid-specific genes in acute megakaryoblastic leukaemia and transient myeloproliferative disorder in Down's syndrome. *British Journal of Haematology*, **90**, 607–614.

James, C., Ugo, V., Le Couedic, J.P., Staerk, J., Delhommeau, F., Lacout, C., Garcon, L., Raslova, H., Berger, R., Bennaceur-Griscelli, A., Villeval, J.L., Constantinescu, S.N., Casadevall, N. & Vainchenker, W. (2005) A unique clonal JAK2 mutation leading to constitutive signaling causes polycythemia vera. *Nature*, **434**, 1144–1148.

Kanezaki, R., Toki, T., Xu, G., Narayanan, R. & Ito, E. (2006) Cloning and characterization of the novel chimeric gene p53/FXR2 in the acute megakaryoblastic leukemia cell line CMK11-5. *Tohoku Journal of Experimental Medicine*, **209**, 169–180.

Kiyoi, H., Yamaji, S., Kojima, S. & Naoe, T. (2007) JAK3 mutations occur in acute megakaryoblastic leukemia both in Down syndrome children and non-Down syndrome adults. *Leukemia*, **21**, 574–576.

Klusmann, J.H., Reinhardt, D., Hasle, H., Kaspers, G.J., Creutzig, U., Hahlen, K., van den Heuvel-Eibrink, M.M. & Zwaan, C.M. (2007) Janus kinase mutations in the development of acute megakaryoblastic leukemia in children with and without Down's syndrome. *Leukemia*, **21**, 1584–1587.

Leonard, W.J. (2000) X-linked severe combined immunodeficiency: from molecular cause to gene therapy within seven years. *Molecular Medicine Today*, **6**, 403–407.

Levine, R.L., Wadleigh, M., Cools, J., Ebert, B.L., Wernig, G., Huntly, B.J., Boggon, T.J., Wlodarska, I., Clark, J.J., Moore, S., Adelsperger, J., Koo, S., Lee, J.C., Gabriel, S., Mercher, T., D'Andrea, A., Frohling, S., Dohner, K., Marynen, P., Vandenberghe, P., Mesa, R.A., Tefferi, A., Griffin, J.D., Eck, M.J., Sellers, W.R., Meyerson, M., Golub, T.R., Lee, S.J. & Gilliland, D.G. (2005) Activating mutation in the tyrosine kinase JAK2 in polycythemia vera, essential thrombocythemia, and myeloid metaplasia with myelofibrosis. *Cancer Cell*, **7**, 387–397.

Miyazaki, T., Kawahara, A., Fujii, H., Nakagawa, Y., Minami, Y., Liu, Z.J., Oihsi, I., Silvennoinen, O., Witthuhn, B.A., Ihle, J.N. & Taniguchi, T. (1994) Functional activation of Jak1 and Jak3 by selective association with IL-2 receptor subunits. *Science*, **266**, 1045–1047.

Morita, S., Kojima, T. & Kitamura, T. (2000) Plat-E: an efficient and stable system for transient packaging of retroviruses. *Gene Therapy*, **7**, 1063–1066.

Mundschau, G., Gurbuxani, S., Gamis, A.S., Greene, M.E., Arceci, R.J. & Crispino, J.D. (2003) Mutagenesis of GATA1 is an initiating event in Down syndrome leukemogenesis. *Blood*, **101**, 4298–4300.

Norton, A., Fisher, C., Liu, H., Wen, Q., Mundschau, G., Fuster, J.L., Hasle, H., Zeller, B., Webb, D.K., O'Marcaigh, A., Sorrell, A., Hilden, J., Gamis, A., Crispino, J.D. & Vyas, P. (2007) Analysis of JAK3, JAK2, and C-MPL mutations in transient myeloproliferative disorder and myeloid leukemia of Down syndrome blasts in children with Down syndrome. *Blood*, **110**, 1077–1079.

Rainis, L., Bercovich, D., Strehl, S., Teigler-Schlegel, A., Stark, B., Trka, J., Amariglio, N., Biondi, A., Muler, I., Rechavi, G., Kempski, H., Haas, O.A. & Izraeli, S. (2003) Mutations in exon 2 of GATA1 are early events in megakaryocytic malignancies associated with trisomy 21. *Blood*, **102**, 981–986.

Russell, S.M., Tayebi, N., Nakajima, H., Riedy, M.C., Roberts, J.L., Aman, M.J., Migone, T.S., Noguchi, M., Markert, M.L., Buckley, R.H., O'Shea, J.J. & Leonard, W.J. (1995) Mutation of Jak3 in a patient with SCID: essential role of Jak3 in lymphoid development. *Science*, **270**, 797–800.

Silvennoinen, O., Witthuhn, B.A., Quelle, F.W., Cleveland, J.L., Yi, T. & Ihle, J.N. (1993) Structure of the murine Jak2 protein-tyrosine kinase and its role in interleukin 3 signal transduction. *Proceedings of the National Academy of Sciences of the United States of America*, **90**, 8429–8433.

Walters, D.K., Mercher, T., Gu, T.L., O'Hare, T., Tyner, J.W., Loriaux, M., Goss, V.L., Lee, K.A., Eide, C.A., Wong, M.J., Stoffregen, E.P., McGreevey, L., Nardone, J., Moore, S.A., Crispino, J., Boggon, T.J., Heinrich, M.C., Deininger, M.W., Polakiewicz, R.D., Gilliland, D.G. & Druker, B.J. (2006) Activating alleles of JAK3 in acute megakaryoblastic leukemia. *Cancer Cell*, **10**, 65–75.

Wechsler, J., Greene, M., McDevitt, M.A., Anastasi, J., Karp, J.E., Le Beau, M.M. & Crispino, J.D. (2002) Acquired mutations in GATA1 in the megakaryoblastic leukemia of Down syndrome. *Nature Genetics*, **32**, 148–152.

Xu, G., Nagano, M., Kanezaki, R., Toki, T., Hayashi, Y., Taketani, T., Taki, T., Mitui, T., Koike, K., Kato, K., Imaizumi, M., Sekine, I., Ikeda, Y., Hanada, R., Sako, M., Kudo, K., Kojima, S., Ohneda, O., Yamamoto, M. & Ito, E. (2003) Frequent mutations in the GATA-1 gene in the transient myeloproliferative disorder of Down's syndrome. *Blood*, **102**, 2960–2968.

Yamashita, Y., Kajigaya, S., Yoshida, K., Ueno, S., Ota, J., Ohmine, K., Ueda, M., Miyazato, A., Ohya, K., Kitamura, T., Ozawa, K. & Mano, H. (2001) Sak serine/threonine kinase acts as an effector of Tec tyrosine kinase. *Journal of Biological Chemistry*, **276**, 39012–39020.

Zhou, Y.J., Chen, M., Cusack, N.A., Kimmel, L.H., Magnuson, K.S., Boyd, J.G., Lin, W., Roberts, J.L., Lengi, A., Buckley, R.H., Geahlen, R.L., Candotti, F., Gadina, M., Changelian, P.S. & O'Shea, J.J. (2001) Unexpected effects of FERM domain mutations on catalytic activity of Jak3: structural implication for Janus kinases. *Molecular Cell*, **8**, 959–969.

Supplementary material

The following supplementary material is available for this article online:

Fig S1. Growth curves of Ba/F3 cells expressing JAK3 mutants in the presence and absence of JAK3 inhibitors. Wild Ba/F3 cells with added IL-3 (A and B) and Ba/F3 cells expressing $JAK3^{Q501H \text{ and } R657Q}$ (C and D), $JAK3^{A572V}$ (E and F), $JAK3^{V674A}$ (G and H), or $JAK3^{I87T}$ (I and J) without added IL-3 were treated with increasing concentrations of JAK3 inhibitor I (A, C, E, G and I) or JAK3 inhibitor II (B, D, F, H and J). Values represent mean ± SD. The experiments were repeated twice, and both data sets were essentially identical.

Table SI. Primer sequences used in the PCR amplification of cDNA and subsequent sequencing.

The material is available as part of the online article from: http://www.blackwell-synergy.com/doi/abs/10.1111/j.1365-2141.2008.07081.x.

(This link will take you to the article abstract).

Please note: Blackwell publishing are not responsible for the content or functionality of any supplementary materials supplied by the authors. Any queries (other than missing material) should be directed to the corresponding author for the article.

Multiplex Reverse Transcription-PCR Screening for *EML4-ALK* Fusion Transcripts

Kengo Takeuchi,[1] Young Lim Choi,[3] Manabu Soda,[3] Kentaro Inamura,[1] Yuki Togashi,[1] Satoko Hatano,[1] Munehiro Enomoto,[3] Shuji Takada,[3] Yoshihiro Yamashita,[3] Yukitoshi Satoh,[2] Sakae Okumura,[2] Ken Nakagawa,[2] Yuichi Ishikawa,[1] and Hiroyuki Mano[3,4]

Abstract

Purpose: EML4-ALK is a fusion-type protein tyrosine kinase that is generated by inv(2)(p21p23) in the genome of non–small cell lung cancer (NSCLC). To allow sensitive detection of *EML4-ALK* fusion transcripts, we have now developed a multiplex reverse transcription-PCR (RT-PCR) system that captures all in-frame fusions between the two genes.

Experimental Design: Primers were designed to detect all possible in-frame fusions of *EML4* to exon 20 of *ALK*, and a single-tube multiplex RT-PCR assay was done with total RNA from 656 solid tumors of the lung ($n = 364$) and 10 other organs.

Results: From consecutive lung adenocarcinoma cases ($n = 253$), we identified 11 specimens (4.35%) positive for fusion transcripts, 9 of which were positive for the previously identified variants 1, 2, and 3. The remaining two specimens harbored novel transcript isoforms in which exon 14 (variant 4) or exon 2 (variant 5) of *EML4* was connected to exon 20 of *ALK*. No fusion transcripts were detected for other types of lung cancer ($n = 111$) or for tumors from 10 other organs ($n = 292$). Genomic rearrangements responsible for the fusion events in NSCLC cells were confirmed by genomic PCR analysis and fluorescence *in situ* hybridization. The novel isoforms of EML4-ALK manifested marked oncogenic activity, and they yielded a pattern of cytoplasmic staining with fine granular foci in immunohistochemical analysis of NSCLC specimens.

Conclusions: These data reinforce the importance of accurate diagnosis of EML4-ALK–positive tumors for the optimization of treatment strategies.

Authors' Affiliations: [1]Division of Pathology, The Cancer Institute, [2]Department of Thoracic Surgical Oncology, Thoracic Center, Cancer Institute Hospital, Japanese Foundation for Cancer Research, Tokyo, Japan; [3]Division of Functional Genomics, Jichi Medical University, Tochigi, Japan; and [4]CREST, Japan Science and Technology Agency, Saitama, Japan

Received 4/19/08; revised 6/23/08; accepted 7/3/08.

Grant support: Grants-in-Aid for Scientific Research from the Ministry of Education, Culture, Sports, Science, and Technology of Japan and grants from the Japan Society for the Promotion of Science; from the Ministry of Health, Labor, and Welfare of Japan; from the National Institute of Biomedical Innovation; from the Smoking Research Foundation; and from the Vehicle Racing Commemorative Foundation.

The costs of publication of this article were defrayed in part by the payment of page charges. This article must therefore be hereby marked *advertisement* in accordance with 18 U.S.C. Section 1734 solely to indicate this fact.

Note: Supplementary data for this article are available at Clinical Cancer Research Online (http://clincancerres.aacrjournals.org/).

K. Takeuchi and Y.L. Choi contributed equally to this work.

Current address for Y. Satoh: Department of Thoracic Surgery, Kitasato University School of Medicine, Kanagawa 228-8520, Japan.

The nucleotide sequences of the *EML4-ALK* variant 4, 5a, and 5b cDNAs have been deposited in DDBJ/EMBL/Genbank under the accession numbers AB374363, AB374364, and AB374365, respectively.

Requests for reprints: Kengo Takeuchi, Division of Pathology, The Cancer Institute, Japanese Foundation for Cancer Research, Tokyo 135-8550, Japan. Phone: 81-3-3520-0111; Fax: 81-3-3570-0558; E-mail: kentakeuchi-tky@umin.net.

doi:10.1158/1078-0432.CCR-08-1018

Chromosome rearrangement is a major mechanism giving rise to transforming potential in human cancers, especially in hematologic malignancies (1). A balanced translocation between chromosomes 9 and 22, for instance, generates an activated protein tyrosine kinase, BCR-ABL, that plays an essential role in the pathogenesis of chronic myeloid leukemia (2). The gene for another protein tyrosine kinase, ALK, is fused to those for NPM1 or other partner proteins in anaplastic lymphoma and soft tissue tumors, resulting in an increase in the kinase activity of ALK (3).

Mitelman et al. have suggested that chromosome translocations, in addition to being common in hematologic malignancies, are not rare in epithelial tumors (4, 5). These researchers also proposed that the genetic mechanisms underlying oncogenesis might not differ fundamentally between hematologic and epithelial malignancies, and that the current apparent difference in the frequency of chromosomal translocations between these two types of cancer is likely to disappear with the advent of new and more powerful investigative tools.

Consistent with this notion, recurrent chromosome rearrangements involving genes for ETS transcriptional factors have been identified in many cases of prostate cancer and may contribute to the hypersensitivity of prostate cancer cells to androgens (6, 7). In addition, we recently discovered another

Translational Relevance

EML4-ALK is a fusion-type protein-tyrosine kinase generated through a recurrent chromosome rearrangement, inv(2)(p21p23), observed in non–small cell lung cancer (NSCLC). Because both *EML4* and *ALK* genes are mapped to the short arm of chromosome 2 in opposite orientations, PCR with primer sets flanking the fusion points of the two genes would not produce any specific products from cells without inv(2)(p21p23). Reverse transcription (RT)-PCR for the fusion point would, therefore, become a highly sensitive and accurate means to detect tumors positive for *EML4-ALK*. Such analyses may detect small amounts of cancer cells in sputa from individuals with NSCLC at early clinical stages. Because several isoforms have been already reported for *EML4-ALK*, it is mandatory to detect all isoforms of the fusion kinase in a sensitive and reliable way. Toward this goal, we here developed a single-tube multiplex RT-PCR screening system to capture all possible isoforms of EML4-ALK. Examination of various tumor samples (n = 656) with our multiplex RT-PCR has indeed identified 11 specimens positive for the variants of EML4-ALK only among lung adenocarcinoma (n = 253). Our system, thus, paves a way for a sensitive molecular detection of this intractable disorder at early curable stages.

recurrent chromosome translocation in non–small cell lung cancer (NSCLC; ref. 8), a major cause of cancer deaths in humans. A small inversion within the short arm of chromosome 2, inv(2)(p21p23), was found to be present in <10% of NSCLC cases and to give rise to a novel fusion-type tyrosine kinase, EML4-ALK, that exhibited marked transforming activity *in vitro* (8). Transgenic mice that specifically express EML4-ALK in lung epithelial cells were also found to develop hundreds of adenocarcinoma nodules in both lungs at only a few weeks after birth, and such nodules disappeared rapidly in response to oral administration of a specific inhibitor of the catalytic activity of ALK.[5] These data thus indicate that EML4-ALK plays a pivotal role in malignant transformation in lung cancer, and they suggest that chemical compounds that inhibit the tyrosine kinase activity of EML4-ALK may provide an effective treatment for EML4-ALK–positive lung cancer. The selection of suitable drugs for individuals with lung cancer will thus require accurate determination of the absence or presence of the *EML4-ALK* fusion gene in biopsy specimens.

Given that *EML4* and *ALK* map in opposite orientations within the short arm of chromosome 2, reverse transcription-PCR (RT-PCR) analysis with primers designed to amplify the fusion points of *EML4-ALK* transcripts would not be expected to yield specific products from normal cells or cancer cells without inv(2)(p21p23). Such analysis should thus provide a highly reliable and sensitive means to detect *EML4-ALK* in clinical specimens. Given that sputum has been shown to be a suitable specimen for such molecular diagnosis of *EML4-ALK* positivity (8), detection of *EML4-ALK*–positive cells by RT-PCR analysis of sputa may be effective for the identification of lung cancer at early clinical stages. The accurate diagnosis of *EML4-ALK*–positive tumors, however, will require that all isoforms of *EML4-ALK* are detected.

The fusion of intron 13 or 20 of *EML4* to intron 19 of *ALK* gives rise to variant 1 or 2 of *EML4-ALK*, respectively (8). We have recently discovered another isoform (variant 3) of *EML4-ALK* in which intron 6 of *EML4* is ligated to intron 19 of *ALK* (9). Theoretically, in addition to such fusion of exons 6, 13, and 20 of *EML4*, an in-frame fusion to exon 20 of *ALK* can occur with exons 2, 18, or 21 of *EML4*. Given that the amino-terminal coiled-coil domain of EML4 is responsible for the dimerization and constitutive activation of EML4-ALK (8) and that exon 2 of *EML4* encodes the entire coiled-coil domain, all of these possible fusion genes would encode EML4-ALK proteins containing the coiled-coil domain and therefore likely produce oncogenic EML4-ALK kinases.

To establish a highly sensitive and accurate PCR-based screening system for *EML4-ALK*–positive cancer, we have now developed a high-throughput multiplex RT-PCR assay for the detection of all potential *EML4-ALK* in-frame fusion transcripts. Among a consecutive series of lung adenocarcinoma specimens (n = 253) as well as other solid tumor samples (n = 403), we have now identified a total of 11 lung adenocarcinoma specimens positive for *EML4-ALK*, two of which harbor previously unidentified fusion mRNAs.

Materials and Methods

Clinical samples and RNA extraction. This study was done with clinical samples from 253 lung adenocarcinomas, 90 other NSCLCs (71 squamous cell carcinomas, 7 adenosquamous carcinomas, 7 large cell carcinomas, 2 pleomorphic carcinomas, and 3 large cell endocrine carcinomas), 21 small cell lung carcinomas, 50 breast carcinomas, 46 renal cell carcinomas, 48 colon carcinomas, 13 prostate carcinomas, 29 urothelial carcinomas, 33 gastric carcinomas, 10 uterine carcinomas, 9 hepatocellular carcinomas, 8 pancreatic carcinomas, and 46 malignant fibrous histiocytomas. All specimens were collected with the approval of the ethical committee at the Cancer Institute Hospital (Tokyo, Japan) and with the informed consent of individuals undergoing surgery from May 1995 to July 2003. The NSCLC cases were consecutive and spanned a period of 19 mo. Histologic diagnosis of NSCLC was made according to the WHO classification (10). All lesions were grossly dissected, rapidly frozen in liquid nitrogen, and stored at -80°C until RNA extraction with an RNeasy Mini Kit (Qiagen). RNA quality and the absence of contamination with genomic DNA were verified by formaldehyde-agarose gel electrophoresis.

Multiplex RT-PCR analysis and nucleotide sequencing. Total RNA was subjected to RT with random primers and SuperScript III reverse transcriptase (Invitrogen). For detection of *EML4-ALK* fusion cDNAs, multiplex PCR analysis was done with AmpliTaq Gold DNA polymerase (Applied Biosystems), the forward primers EML4 72F (5′-GTCAGCTCTTGAGTCACGAGTT-3′) and Fusion-RT-S (5′-GTGCAGTGTTTAGCATTCTTGGGG-3′), and the reverse primer ALK 3078RR (5′-ATCCAGTTCGTCCTGTTCAGAGC-3′). The *GAPDH* cDNA was amplified by PCR with the primers 5′-GTCAGTGGTGGACCT-GACCT-3′ and 5′-TGAGCTTGACAAAGTGGTCG-3′. For amplification of *EML4-ALK* fusion cDNAs, the samples were incubated at 94°C for 10 min and then subjected to 35 cycles of denaturation at 94°C for 1 min, annealing at 64°C for 1 min, and polymerization at 72°C for 1 min. For amplification of *GAPDH* cDNA, the samples were subjected to 35 cycles of 94°C for 1 min, 58°C for 30 s, and 72°C for 30 s. Virtual gel electrophoresis of multiplex RT-PCR products was done with a 2100 Bioanalyzer (Agilent Technologies).

[5] M. Soda et al., submitted for publication.

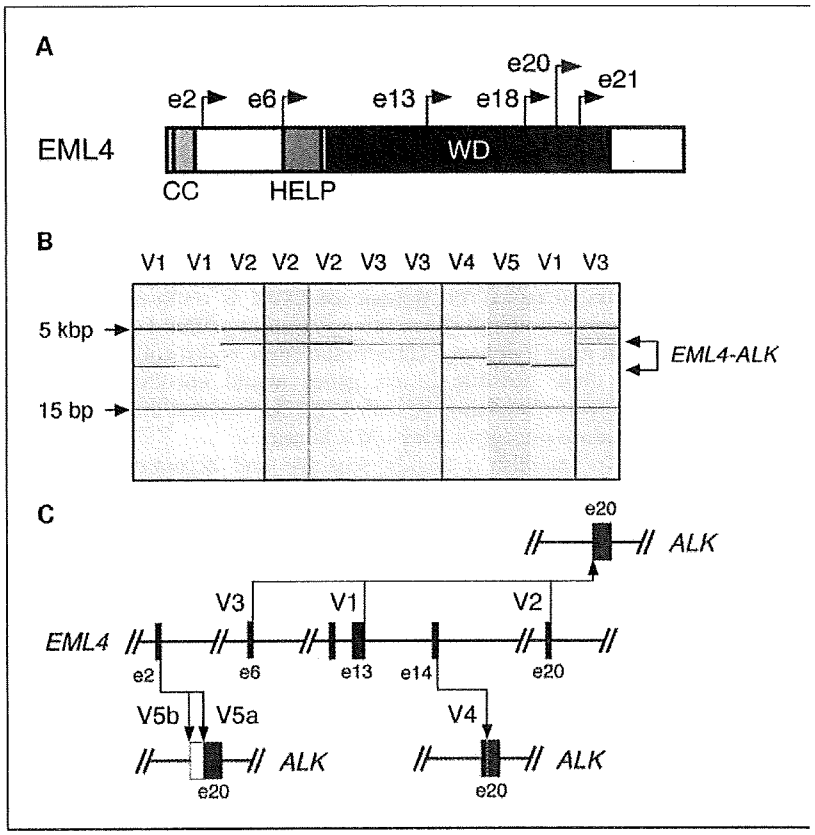

Fig. 1. Identification of *EML4-ALK* variants 4 and 5. *A*, schematic representation of the structure of EML4. The corresponding positions of exons (*e*) that can theoretically be fused in-frame to exon 20 of *ALK* are indicated by arrows, with known fusion points being denoted in red. CC, coiled-coil domain; HELP, hydrophobic EMAP (echinoderm microtubule-associated protein) – like protein domain; WD, WD repeats. *B*, virtual gel electrophoresis of multiplex RT-PCR products derived from lung adenocarcinoma specimens. Seven samples (*blue*) were known to harbor *EML-ALK* variants (*V*) 1, 2, or 3, whereas four samples were newly detected by multiplex RT-PCR. Two of the latter four specimens yielded PCR products corresponding to the newly identified variants 4 and 5. The positions of the fusion products of *EML4-ALK* are indicated on the right, and those of DNA size standards (5 kbp and 15 bp) are shown on the left. *C*, fusions between exons of *EML4* and *ALK*. Fusion of exons 6, 13, or 20 of *EML4* to exon 20 of *ALK* gives rise to variants 3, 1, and 2 of *EML4-ALK*, respectively. In addition, nucleotide sequencing of the PCR products shown in *B* revealed that exon 14 or 2 of *EML4* was fused to exon 20 of *ALK* in the cDNAs for *EML4-ALK* variants 4 and 5, respectively.

The primers used for direct amplification of the fusion points of individual cDNAs were 5′-AGGAGAGAACTCAGCGACACTACC-3′ and 5′-TCCACGCTCAAAAGTGCCAAGTCC-3′ for variant 4 and 5′-GCTTTCCCCGCAAGATGGACGG-3′ and 5′-AGCTTGCTCAGCTTG-TACTCAGGG-3′ for variant 5. Full-length cDNAs for *EML4-ALK* variants were amplified with PrimeSTAR DNA polymerase (Takara Bio) and the primers 5′-ACTCTGTCGGTCCGCTGAATGAAG-3′ and 5′-CCACGGTCTTAGGGATCCCAAGG-3′.

Fluorescence in situ *hybridization analysis.* Surgically resected lung cancer tissue was fixed in 20% formalin, embedded in paraffin, sectioned at a thickness of 4 μm, and placed on glass slides. The unstained sections were processed with a Histology FISH Accessory Kit (Dako), subjected to hybridization with fluorescently labeled bacterial artificial chromosome clone probes for *EML4* and *ALK* (GSP Laboratory) or for genomic regions upstream and downstream of the *ALK* break point (Dako), stained with 4,6-diamidino-2-phenylindole, and examined with a fluorescence microscope (BX51; Olympus).

Immunohistochemical analysis. Unstained paraffin-embedded sections were depleted of paraffin with xylene, rehydrated with a graded series of ethanol solutions, and then subjected to heat-induced antigen retrieval with Target Retrieval Solution pH 9.0 (Dako) before immunohistochemical staining with a mouse monoclonal antibody to ALK (ALK1, Dako) at a dilution of 1:20. Immune complexes were detected with the use of an EnVision+DAB system (Dako) with minor modifications.[6]

Transforming potential of EML4-ALK proteins. Protein analysis of EML4-ALK variants was done as described previously (8). In brief, the *EML4-ALK* variant 4, 5a, or 5b cDNAs were fused with an oligonucleotide encoding the FLAG epitope tag and inserted into the retroviral expression plasmid pMXS (11). The resulting plasmids and similar pMXS-based expression plasmids for EML4-ALK variant 1, variant 1(K589M), variant 2, variant 3a, and variant 3b were individually introduced into HEK293 cells. Lysates of the transfected cells were subjected to immunoprecipitation with antibodies to FLAG, and the resulting precipitates were subjected either to immunoblot analysis with the same antibodies or to an *in vitro* kinase assay with the YFF peptide (12). Mouse 3T3 fibroblasts were also infected with recombinant retroviruses for each of the EML4-ALK variants or wild-type ALK and were then cultured for 12 d for a focus formation assay. The same set of 3T3 cells was injected s.c. into nu/nu mice, and tumor formation was examined after 20 d.

Results

Multiplex RT-PCR screening for EML4-ALK fusion transcripts in lung adenocarcinoma. As described above, exons 2, 6, 13, 18, 20, and 21 of *EML4* may participate in an in-frame fusion to exon 20 of *ALK* (Fig. 1A). To identify all possible *EML4-ALK* fusion cDNAs in a single-tube experiment, we designed a mixture of two sense primers (one targeted to exon 2 and the other to exon 13 of *EML4*) and a single antisense primer (targeted to exon 20 of *ALK*) and did multiplex RT-PCR with these primers and total cDNA preparations from tumor specimens. The exon 2 primer for *EML4* would be expected to generate a PCR product of 458 bp with the exon 2 (*EML4*)-exon 20 (*ALK*) fusion cDNA or of 917 bp with the exon 6-exon 20 fusion cDNA (variant 3). In addition, the exon 13 primer for *EML4* would be expected to generate PCR products of 432, 999, 1,185, or 1,284 bp with the exon 13-exon 20 (variant 1), exon 18-exon 20, exon 20-exon 20 (variant 2), and exon 21-exon 20 fusion cDNAs, respectively.

[6] K. Takeuchi et al., manuscript in preparation.

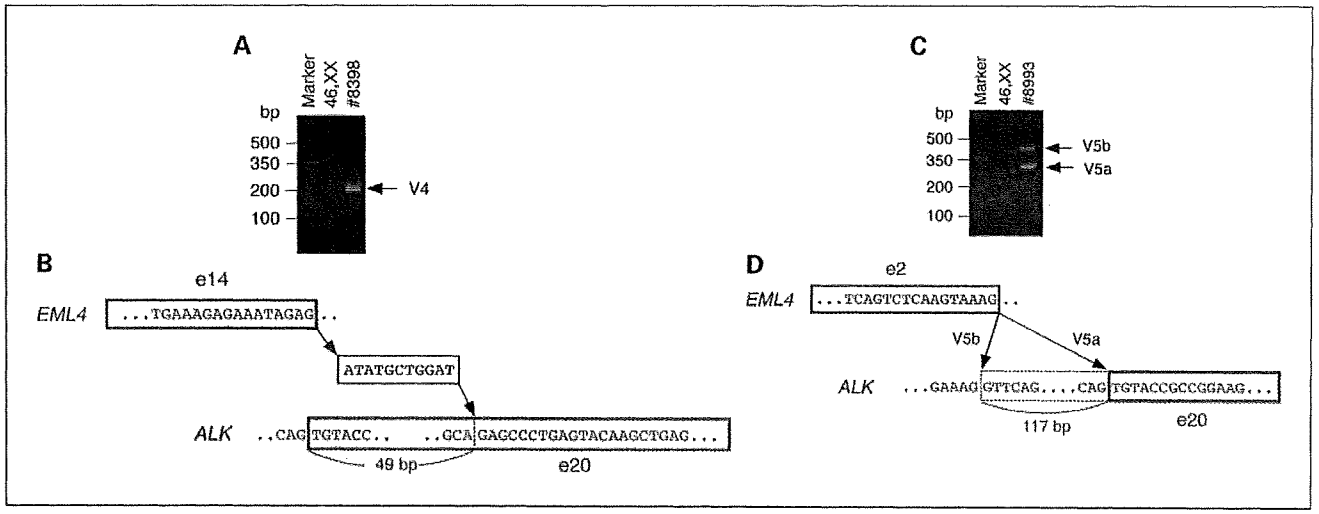

Fig. 2. Structure of *EML4-ALK* variant 4 and 5 cDNAs. *A,* RT-PCR amplification of the fusion point of *EML4-ALK* variant 4 mRNA in NSCLC specimen ID no. 8398 as well as in peripheral blood mononuclear cells of a female volunteer (46,XX). A PCR product of 203 bp corresponding to *EML4-ALK* variant 4 was specifically amplified from the tumor cells. The left lane contains DNA size standards (50-bp ladder). *B,* nucleotide sequencing of the PCR product in *A* revealed that exon 14 of *EML4* (*blue*) was connected to an 11-bp cDNA fragment of unknown identity (*black*), which was ligated in turn to the nucleotide at position 50 of exon 20 of *ALK* (*red*). *C,* RT-PCR amplification of the fusion point of *EML4-ALK* variant 5 mRNA in NSCLC specimen ID no. 8993 as well as in peripheral blood mononuclear cells of a female volunteer (46,XX). Two specific products of 415 and 298 bp were obtained, corresponding to variants 5b and 5a, respectively. The left lane contains DNA size standards (50-bp ladder). *D,* nucleotide sequencing of the PCR products in *C* revealed that exon 2 of *EML4* was fused either to exon 20 of *ALK*, generating the variant 5a cDNA, or to a position 117 bp upstream of exon 20 of *ALK*, generating the variant 5b cDNA.

Virtual gel electrophoresis of the multiplex RT-PCR products (Fig. 1B) revealed that 11 samples (4.35%) were positive for *EML4-ALK* cDNA among a consecutive series of 253 lung adenocarcinoma specimens, including those examined in our previous studies (8, 9, 13). All of the specimens previously shown to harbor *EML4-ALK* (two cases with variant 1, three with variant 2, and two with variant 3) were faithfully detected with our multiplex RT-PCR system. No specific PCR products were obtained for other types of lung cancer (n = 111) or other solid tumors (n = 292). Nucleotide sequencing of the PCR products for the newly identified positive cases revealed that one specimen was positive for variant 1 and another for variant 3 of *EML4-ALK*, but that the remaining two specimens harbored previously unidentified variants (Fig. 1B and C). Exon 14 of *EML4* was ligated to a position within exon 20 of *ALK* in the product from tumor ID no. 8398 (designated variant 4), whereas exon 2 of *EML4* was ligated to exon 20 of *ALK* in the product from tumor ID no. 8993 (designated variant 5).

Structure of EML4-ALK variant 4 cDNA. To verify the presence of novel *EML4-ALK* variants in the cancer cells, we first did direct RT-PCR analysis for the cDNA of tumor ID no. 8398 with a new set of primers encompassing the putative fusion point of variant 4. This analysis showed the presence of the fusion cDNA (Fig. 2A). Nucleotide sequencing of the PCR product revealed that exon 14 of *EML4* was fused to an unknown sequence of 11 bp, which in turn was connected to the nucleotide at position 50 of exon 20 of *ALK* (Fig. 2B). (We failed to detect a region of the human genome (build 36) homologous to the 11-bp connecting sequence in a BLAST search.[7]) Although exon 14 of *EML4* is not expected to produce an in-frame fusion to exon 20 of *ALK*, insertion of the unknown 11-bp sequence and its ligation to a position within the *ALK* exon allows an in-frame connection between the two genes. Fusion cDNAs in which the point of connection is located within, rather that at the 5′ terminus of, exon 20 of *ALK* have also been described for *MSN-ALK* (14) and *MYH9-ALK* (15).

We further examined whether a full-length cDNA encoding such an unexpected EML4-ALK variant could be isolated from the cancer cells. For this purpose, we designed a sense primer targeted to the 5′ untranslated region of *EML4* cDNA as well as an antisense primer targeted to the 3′ untranslated region of *ALK* cDNA. Direct RT-PCR analysis with this primer set yielded a single PCR product of ~3.4 kbp with total cDNA of tumor ID no. 8398 (Supplementary Fig. S1A). Complete nucleotide sequencing of the PCR product revealed that the cDNA contained an open reading frame for 1,097 amino acids comprising residues 1 to 547 of human EML4, residues 1,075 to 1,620 of human ALK, and 4 amino acids of unknown origin between these two sequences (Supplementary Fig. S1B). The isolation of a full-length cDNA containing the 11-bp insert indicated that the variant 4 protein was likely expressed in the cancer cells.

Structure of EML4-ALK variant 5 cDNAs. We similarly investigated the presence of variant 5 mRNA in the cells of tumor ID no. 8993. Direct RT-PCR analysis to amplify the fusion point of this variant cDNA yielded two independent products of 298 and 415 bp (Fig. 2C). Nucleotide sequencing of each product revealed that the former contained exon 2 of *EML4* and exon 20 of *ALK*, as expected, whereas in the latter, exon 2 of *EML4* was connected to a position within intron 19 of *ALK* located 117 bp upstream of exon 20 (Fig. 2D). These fusion constructs were designated variants 5a and 5b, respectively.

Although no mRNAs or expressed sequence tags in the nucleotide sequence database were found to contain the

[7] http://www.ncbi.nlm.nih.gov/genome/seq/blastgen/blastgen.cgi?taxid=9606

117-bp sequence of intron 19 of *ALK*, the human genome sequence surrounding the 5′ terminus of this 117-bp sequence is AG-GT (Fig. 2D), which conforms to the consensus sequence for a splicing acceptor site. To show that such a cryptic exon is indeed involved in the production of an oncogenic kinase, we attempted to detect full-length cDNAs for variants 5a and 5b from total cDNA of tumor ID no. 8993. A doublet of PCR products of ~2.0 kbp was obtained (Supplementary Fig. S1A), and nucleotide sequencing of these products revealed that they indeed encode EML4-ALK variant 5a and 5b proteins (Supplementary Fig. S1C). Genomic PCR and fluorescence *in situ* hybridization (FISH) analyses further revealed that the cells of tumor ID no. 8993 harbor a single *EML4-ALK* fusion gene, suggesting that variant 5a and 5b mRNAs are generated by alternative splicing of the primary transcript of this single fusion gene (see below).

Detection of the EML4-ALK fusion genes by FISH. To confirm the rearrangements involving the *ALK* locus in the specimens harboring variants 4 and 5 of *EML4-ALK* cDNA, we did FISH analysis with tissue sections. We first designed a FISH-based "fusion assay" for *EML4* and *ALK* genes. Bacterial artificial chromosome fragments encompassing the entire genes were fluorescently labeled green and red, respectively. An overlapping signal for both probes was readily identified in a merged image for the tumor cells harboring variants 4 or 5 of *EML4-ALK* (Fig. 3A). To confirm further the breakage of the *ALK* locus, we did an "*ALK* split assay" with bacterial artificial chromosome fragments encompassing the 5′ or 3′ regions of the locus and labeled green and red, respectively. In this assay, the normal *ALK* locus would be expected to yield an overlapping signal, whereas a pair of separate green and red signals would indicate genomic breakage within *ALK*. As expected, a proportion of cells of tumor ID no. 8398 or no. 8993 in the histologic sections generated one overlapping signal and one pair of split signals (Fig. 3B), suggesting that these tumor cells each have at least one normal and at least one rearranged *ALK* locus.

These data, together with genomic PCR analysis (data not shown), thus indicated that the cells of each of these tumors harbor one normal chromosome 2 and a chromosome 2 with an inv(2)(p21p23) rearrangement. The other *EML4-ALK* cDNA-positive specimens (variants 1 to 3) in this cohort showed a similar FISH labeling profile, consistent with the presence of the corresponding *EML4-ALK* rearrangements (data not shown).

***Detection of EML4-ALK proteins* in situ.** To detect EML4-ALK proteins in the cancer cells, we did immunohistochemical analysis with the ALK1 monoclonal antibody to ALK (16). The cytoplasm of tumor cells harboring *EML4-ALK* variant 1 (ID no. 9034), variant 4 (ID no. 8398), or variant 5 (ID no. 8993) manifested a diffuse pattern of immunoreactivity with fine granular concentrations (Fig. 3C). No normal pulmonary epithelial cells or lymphocytes in the sections of these specimens reacted with the antibody.

Transforming activity of EML4-ALK variants. We prepared expression plasmids for FLAG epitope-tagged EML4-ALK variants 1, 2, 3a, 3b, 4, 5a, and 5b, the predicted molecular sizes of which are 118,356; 146,913; 87,613; 88,874; 122,541; 71,046; and 74,867 Da, respectively. Each of these proteins, as well as a kinase-inactive mutant of EML4-ALK variant 1 (8), was expressed independently in HEK293 cells, immunoprecipitated, and subjected to immunoblot analysis with antibodies to FLAG. Each cDNA generated an EML4-ALK protein of the expected molecular size (Fig. 4A). The same immunoprecipitates were subjected to an *in vitro* kinase assay with the synthetic peptide YFF (12). Each variant protein (with the exception of the kinase-inactive mutant of variant 1) was shown to possess protein tyrosine kinase activity, with that of variants 3a, 3b, and 5b being most prominent (Fig. 4A).

To examine the transforming potential of the EML4-ALK variants, we transfected mouse 3T3 fibroblasts with the corresponding expression plasmids and then cultured the cells for 12 days. Transformed foci were readily detected for the cells expressing the variants of EML4-ALK but not for cells overexpressing wild-type ALK (Fig. 4B). Furthermore, s.c. injection of the transfected 3T3 cells into the shoulder of nude mice revealed that those expressing the various EML4-ALK isoforms, but not those overexpressing wild-type ALK, formed large tumors *in vivo* (Fig. 4B).

Discussion

We have done multiplex RT-PCR analysis to detect all possible isoforms of *EML4-ALK* transcripts in NSCLC cells, and unexpectedly identified two novel subtypes of the fusion event. This finding was supported by detection of the corresponding fusion genes by genomic PCR and FISH

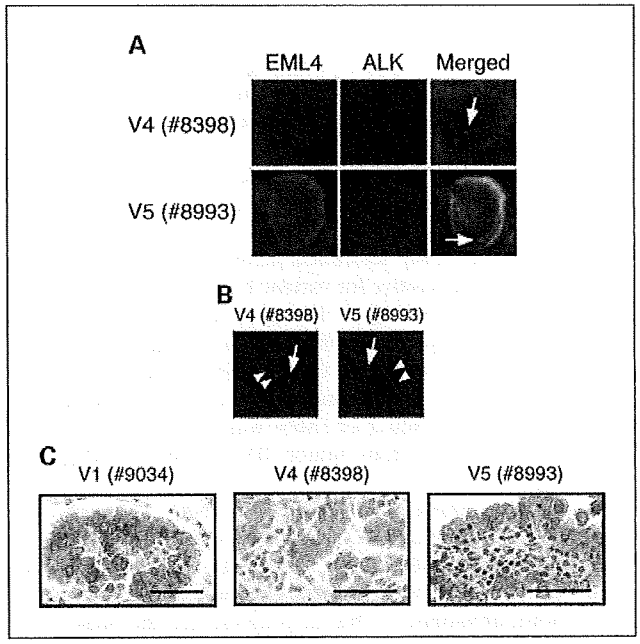

Fig. 3. FISH and immunohistochemical analyses of NSCLC specimens. *A*, FISH analysis of representative cancer cells in sections of lung adenocarcinoma harboring *EML4-ALK* variant 4 (ID no. 8398) or variant 5 (ID no. 8993). Each section was subjected to hybridization with differentially labeled probes for *EML4* (*left*) or for *ALK* (*center*). A fusion signal (*arrow*) and a pair of green (*EML4*) and red (*ALK*) signals are present in each merged image (*right*). *B*, the same clinical specimens as in *A* were subjected to FISH analysis with differentially labeled probes for the 5′ (*green*) or 3′ (*red*) regions of the *ALK* locus. A pair of split signals (*arrowheads*) and an overlapping signal (*arrow*) indicate the rearranged and normal *ALK* loci, respectively. *C*, immunohistochemical analysis of NSCLC specimens positive for *EML4-ALK* variants 1 (ID no. 9034), 4 (ID no. 8398), or 5 (ID no. 8993) with a monoclonal antibody to ALK. A pattern of diffuse staining with fine granular foci was apparent in the cytoplasm of all three tumors. Scale bars, 50 μm.

analyses and by that of the encoded proteins by immunohistochemical analysis in the NSCLC cells. Together with the previously isolated variants (8, 9), we have to date identified a total of seven distinct isoforms of EML4-ALK (variants 1, 2, 3a, 3b, 4, 5a, and 5b). Given that each of these isoforms possesses marked transforming activity, they all likely play an important role in the development of NSCLC. Our failure to detect *EML4-ALK* cDNA in the other solid tumors (n = 313) examined suggests that *EML4-ALK* may be an oncogene specific to NSCLC, especially to lung adenocarcinoma.

In our multiplex RT-PCR analysis, a sense primer targeted to exon 2 of *EML4* was designed to detect fusion events involving exon 2 or 6 of *EML4*, and PCR products of the expected sizes were indeed obtained with NSCLC specimens positive for such fusion events (variants 5 and 3, respectively). The other sense primer was targeted to exon 13 of *EML4* and was designed to detect fusion events involving exon 13, 18, 20, or 21 of *EML4*. Given that we were able to readily amplify a specific product of 1185 bp corresponding to the fusion event involving exon 20 of *EML4* (variant 2), it is likely that all possible fusions giving rise to PCR products up to this size would have been detected in our cohort. It should be noted, however, that a possible fusion between exon 21 of *EML4* and exon 20 of *ALK* would be expected to generate a PCR product of 1,284 bp. Although the size difference between the 1,185- and 1,284-bp products is small (99 bp), it is still possible that our multiplex RT-PCR analysis failed to efficiently amplify the longer product and that there may be as-yet-undetected fusion events for *EML4-ALK* in our cohort.

All EML4-ALK isoforms manifested a similar subcellular distribution profile despite marked differences in the size and domain structure of the EML4 portions of these chimeric proteins. In addition, the intracellular signaling systems activated by EML4-ALK may be shared among variants 1 to 5 (Supplementary Fig. S2). The EML4 portion of variant 5 comprises only the coiled-coil domain. This domain of EML4 may therefore play an essential role not only in the dimerization and activation of EML4-ALK isoforms (8) but also in tethering EML4-ALK to specific subcellular components. The pattern of subcellular immunostaining for EML4-ALK (cytoplasmic staining with fine granular foci) was distinct from that for other ALK fusion proteins associated with other malignancies (17, 18), suggesting that the subcellular localization of ALK fusion kinases varies substantially. The first such fusion kinase to be identified, NPM-ALK, preferentially phosphorylates STAT3, which is thought to participate in mitogenic signaling by NPM-ALK (19–21). Five ALK fusion kinases (NPM-ALK, TFG-ALK, ATIC-ALK, TPM3-ALK, and CLTC-ALK) were shown to differ markedly in their abilities to transform 3T3 fibroblasts, to phosphorylate STAT3 and AKT, and to activate phosphoinositide 3-kinase (17). Furthermore, a proteomics approach to identify tyrosine-phosphorylated proteins failed to detect marked phosphorylation of STAT3 in NSCLC specimens positive for EML4-ALK (22). It is therefore likely that each ALK fusion kinase exerts its effects through fusion-specific (although possibly partially overlapping) downstream pathways. In addition, we detected slight differences in catalytic and transforming activities among the variants of EML4-ALK (Fig. 4). These differences are likely due to the different portions of EML4 present in the different variants, which may affect dimerization affinity or the recruitment of substrates.

In addition to *EML4-ALK*, NSCLC cells harbor other potent oncogenes such as mutant versions of *EGFR* or *KRAS*. These three oncogenes, however, were found to be mutually exclusive

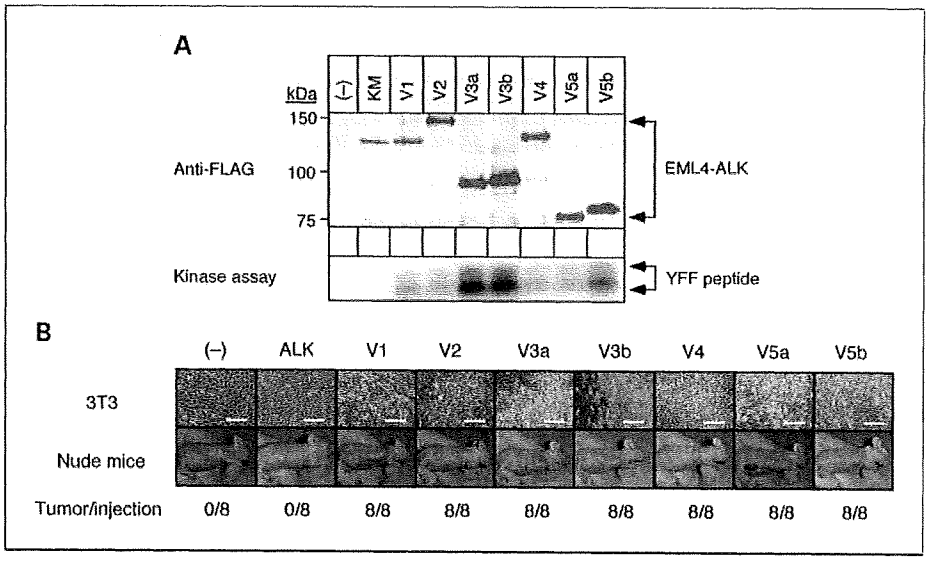

Fig. 4. Transforming potential of EML4-ALK variants. *A*, HEK293 cells expressing FLAG-tagged variant 1, 2, 3a, 3b, 4, 5a, or 5b of EML4-ALK were lysed and subjected to immunoprecipitation with antibodies to FLAG. The resulting precipitates were then either subjected to immunoblot analysis with antibodies to FLAG (*top*) or assayed for kinase activity with the synthetic YFF peptide (*bottom*). Cells transfected with the empty vector (-) or with a vector for a kinase-inactive mutant (*KM*) of EML4-ALK variant 1 were also analyzed. The positions of molecular size standards (kDa) and of EML4-ALK proteins are indicated on the left and right of the top panel, respectively. *B*, mouse 3T3 fibroblasts were transfected with expression plasmids for wild-type ALK or FLAG-tagged EML4-ALK variants, or with the empty plasmid (-), and were photographed after culture for 12 d (*top*). Scale bars, 200 μm. Alternatively, the transfected cells were injected s.c. into the shoulder of nu/nu mice and tumor formation was examined after 20 d (*bottom*). The number of tumors formed per eight injections is indicated at the bottom.